NRC Research Press

ARTICLE

Dental anatomy of the apex predator *Sinraptor dongi* (Theropoda: Allosauroidea) from the Late Jurassic of China

Christophe Hendrickx, Josef Stiegler, Philip J. Currie, Fenglu Han, Xing Xu, Jonah N. Choiniere, and Xiao-Chun Wu

Abstract: The dental morphology of the holotype of the theropod *Sinraptor dongi* from the Jurassic Shishugou Formation of China is comprehensively described. We highlight a combination of dental features that appear to be restricted to *Sinraptor*: (*i*) crowns with denticulated mesial and distal carinae extending from the root and an irregular surface texture on the enamel; (*ii*) a D- to salinon-shaped cross-sectional outline at the crown base in mesialmost teeth; (*iii*) mesial crowns with mesial carinae spiraling mesiolingually and lingually positioned longitudinal groove adjacent to the mesial carina; and (*iv*) particularly labiolingually compressed lateral teeth with weakly labially deflected distal carinae, flat to concave basocentral surfaces of the labial margins of the crowns, and horizontally elongated distal denticles showing short to well-developed interdenticular sulci. Using cladistic, multivariate, discriminant, and cluster analyses, we demonstrate that the dentition of *Sinraptor* is relatively similar to that of ceratosaurids, megalosauroids, and other allosauroids and is particularly close to that of *Allosaurus*. The dental anatomy of *Sinraptor* and *Allosaurus*, which differs mainly in the labiolingual compression of the lateral crowns and in the number of premaxillary teeth, shows adaptations towards a predatory lifestyle, including premaxillary teeth capable of enduring tooth-to-bone contact and crowns with widely separated mesial and distal carinae capable of inflicting widely open wounds.

Key words: tooth, crown, denticle, dinosaur, theropod.

Résumé : La morphologie dentaire de l'holotype du théropode *Sinraptor dongi* de la Formation jurassique de Shishugou, en Chine, est décrite de manière exhaustive. Nous soulignons une combinaison de caractères dentaires qui semblent être exclusifs à *Sinraptor*, dont (*i*) des couronnes présentant des carènes mésiales et distales s'étendant jusqu'à la racine, et une texture de l'émail irrégulière, (*ii*) une section transversale de la base de la couronne des dents les plus mésiales en forme de D ou de salinon, (*iii*) des carènes mésiales des couronnes mésiales spiralant mésiolingualement et un sillon longitudinal adjacent à la carène mésiale sur la surface linguale et (*iv*) des dents latérales particulièrement comprimées labiolingualement présentant des carènes distales faiblement déviées labialement, des surfaces basocentrales plates à concaves des marges labiales des couronnes et des denticules distaux allongés horizontalement montrant des sulcus interdenticulaires courts à bien développés. En utilisant des analyses cladistiques, multivariées, discriminantes et typologiques, nous démontrons que la dentition de *Sinraptor* est assez semblable à celle des cératosauridés, des mégalosauroïdes et d'autres allosauroïdes, et est particulièrement proche de celle d'*Allosaurus*. L'anatomie dentaire de *Sinraptor* et d'*Allosaurus*, dont la principale différence est la compression labiolinguale des couronnes latérales et le nombre de dents prémaxillaires, présente des adaptations à un mode de vie prédateur, dont des dents prémaxillaires résistantes aux contacts dent-à-os et des couronnes présentant des carènes mésiales et distales largement séparées pouvant infliger de larges blessures ouvertes. [Traduit par la Rédaction]

Mots-clés : dent, couronne, denticule, dinosaure, théropode.

Introduction

Sinraptor dongi Currie and Zhao, 1993 was one of the apex terrestrial carnivores in the vertebrate ecosystem of the "upper" Shishugou Formation, Xinjiang Uygur Autonomous Region, Xinjiang Province, northwestern China (Currie and Zhao 1993; Xu and Clark 2008; Fig. 1A (3)). The formation has yielded one of most diverse dinosaur faunas from the Jurassic of Asia and is currently divided into lower, middle, and upper beds (Choiniere et al. 2014*a*, 2014*b*; Moore et al. 2018). The upper section of the Shishugou Formation (here referred as the "upper" Shishugou Formation), which includes the upper part of the middle beds and the upper beds (Fig. 1A), is the richest taxonomically, with a dozen dinosaur species recorded to date (Currie and Zhao 1993; Eberth et al. 2010;

Received 2 December 2019. Accepted 14 February 2020.

C. Hendrickx* and J.N. Choiniere. Evolutionary Studies Institute, University of the Witwatersrand, Private Bag 3, Johannesburg WITS 2050, South Africa.
J. Stiegler. Department of Biological Sciences, The George Washington University, Washington, DC 20052, USA.
P.J. Currie. Department of Biological Sciences, University of Alberta, Edmonton, AB T6G 2E9, Canada.
F. Han. School of Earth Sciences, China University of Geosciences, Wuhan, China.
X. Xu. Key Laboratory of Vertebrate Evolution and Human Origins, Institute of Vertebrate Paleontology and Paleoanthropology, Chinese Academy of Sciences, 142 Xiwai Street, Beijing 100044, China; Chinese Academy of Sciences Center for Excellence in Life and Paleoenvironment, 142 Xiwai Street, Beijing 100044, China.
X.-C. Wu. Canadian Museum of Nature, P.O. Box 3443, Station 'D', Ottawa, ON K1P 6P4, Canada.
Corresponding author: Christophe Hendrickx (email: christophendrickx@gmail.com).
*Present address: Unidad Ejecutora Lillo, CONICET-Fundación Miguel Lillo, Miguel Lillo 251, San Miguel de Tucumán 4000, Tucumán, Argentina.

Fig. 1. Stratigraphy and dinosaur component from the middle and upper beds of the Shishugou Formation and incomplete skull of *Sinraptor dongi*. (A) Stratigraphic section of Oxfordian deposits of the Shishugou Formation (composite section modified from Eberth et al. (2010) and Moore et al. (2018)) and dinosaurian composition of the Oxfordian part of the Shishugou Formation. T-BW and T-1 show the stratigraphic positions and ages of two radiometrically dated volcanic tuffs in a section of the Shishugou Formation at Wucaiwan. Herbivorous and faunivorous dinosaurs are in green and red, respectively. Dinosaurs not to scale. 1, the stegosaur *Jiangjunosaurus junggarensis*; 2, the alvarezsauroid *Haplocheirus sollers*; 3, the metriacanthosaurid *Sinraptor dongi*; 4, the eusauropod *Bellusaurus sui*; 5, the alvarezsauroid *Aorun zhaoi*; 6, the coelurosaur *Zuolong salleei*; 7, the mamenchisaurid *Tienshanosaurus chitaiensis*; 8, the alvarezsauroid *Shishugounykus inexpectus*; 9, the proceratosaurid *Guanlong wucaii*; 10, the ornithischian *Gongbusaurus wucaiwanensis*; 11, the ceratopsian *Hualianceratops wucaiwanensis*; 12, the mamenchisaurid *Mamenchisaurus sinocanadorum*; 13, the noasaurid *Limusaurus inextricabilis*; and 14, the marginocephalian *Yinlong downsi*. (B–C) Incomplete skull of *Sinraptor dongi* (IVPP 10600) in plaster jackets, as recovered on site. (B) Right part of cranium and mandible, left premaxilla, left lacrimal, part of left surangular?, skull roof, and braincase. (C) Left part of cranium and mandible, dentary teeth, and right quadrate and quadratojugal. Silhouettes are based on the reconstructions of Cisiopurple (*Aorun*, *Hualianceratops*, *Bellusaurus*, *Jiangjunosaurus*), Scott Hartman (*Guanlong*, *Mamenchisaurus*), Gregory S. Paul (*Yangchuanosaurus* for *Sinraptor*), Choiniere et al. (2010*a*; *Zuolong*), Choiniere et al. (2010*b*; *Haplocheirus*), Wang et al. (2016; *Limusaurus*), Qin et al. (2019; *Shishugounykus*), Megalotitan (*Tienshanosaurus*), and Ornithischophilia (*Yinlong*). [Colour online.]

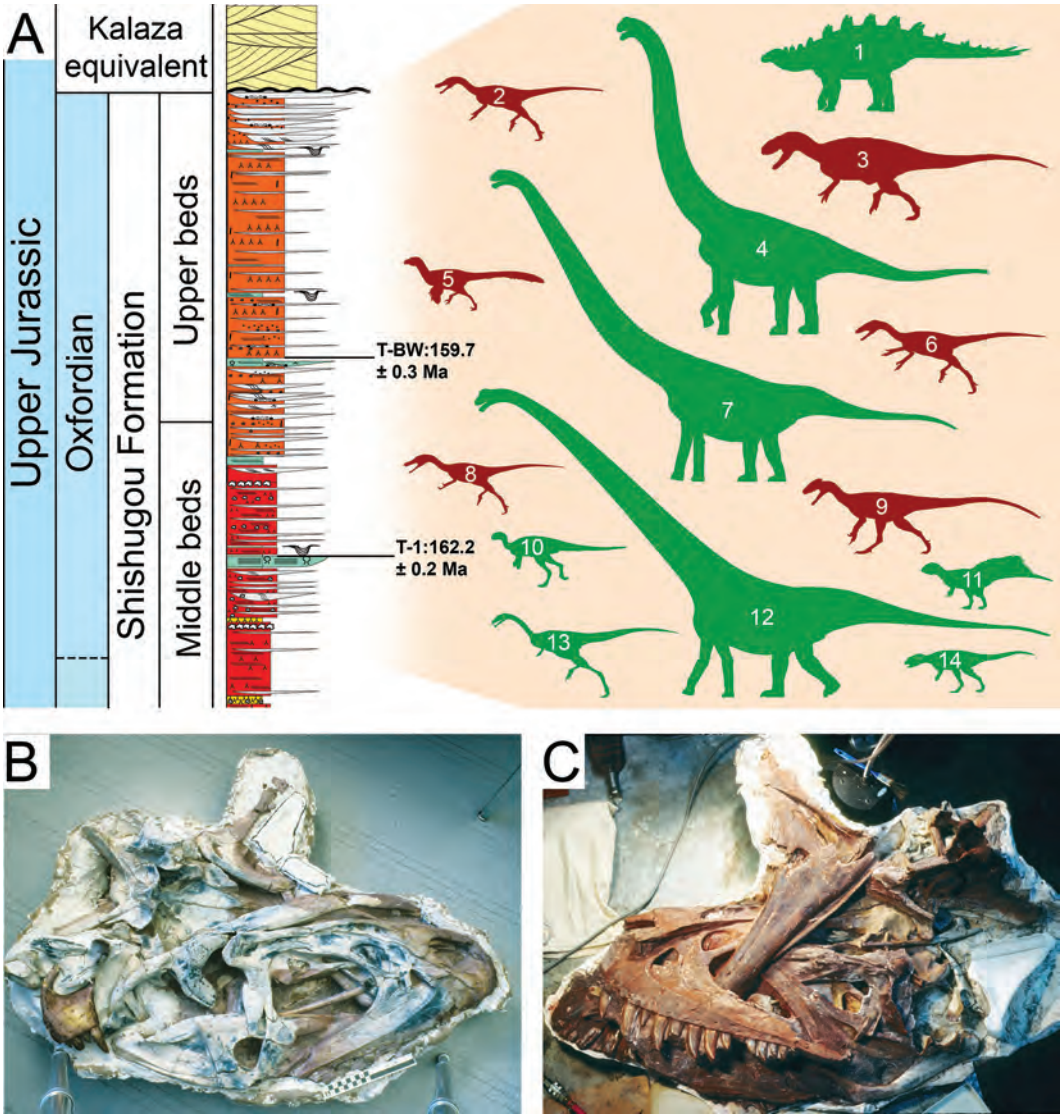

Choiniere et al. 2014*a*, 2014*b*; Qin et al. 2019). The fauna is dominated by herbivorous dinosaurs belonging to five clades (Fig. 1A): Sauropodomorpha with *Mamenchisaurus sinocanadorum* Russell and Zheng,1993; *Tienshanosaurus chitaiensis* Young, 1937; and *Bellusaurus sui* Dong, 1990 (and see Dong 1992; Moore et al. 2018); Theropoda with *Limusaurus inextricabilis* Xu et al., 2009 (and see Wang et al. 2016, 2017); Ornithischia clade indet. With *Gongbusaurus wucaiwanensis* Dong, 1989; Stegosauria with *Jiangjunosaurus junggarensis* Jia et al., 2007; and Marginocephalia with *Yinlong downsi* Xu et al., 2006*b* (and see Han et al. 2016, 2018); and *Hualianceratops wucaiwanensis* Han et al., 2015. In addition to the large-bodied predator *Sinraptor dongi* (i.e., approximately 7 m in length; Tanke and Currie 1998), carnivorous theropods are represented by five small- to medium-sized dinosaurs (Fig. 1A): the basally branching coelurosaur *Zuolong salleei* Choiniere et al., 2010*a*; the proceratosaurid tyrannosauroid *Guanlong wucaii* Xu et al., 2006*a*; and the early alvarezsauroids *Aorun zhaoi* Choiniere et al., 2014*a* (and see Xu et al. 2018), *Haplocheirus sollers* Choiniere et al., 2010*b* (and see

Fig. 2. Stratigraphic distribution of averostran theropods and cranial and skeletal reconstructions of the metriacanthosaurid *Sinraptor dongi* (IVPP 10600). (A) Stratigraphically calibrated phylogeny of Ceratosauria, Megalosauroidea, Allosauroidea, and Coelurosauria, with metriacanthosaurid clades and taxa in red (dashed lines represent the phylogenetic position of the putative metriacanthosaurid *Erectopus superbus*; phylogeny based on the results of Carrano et al. 2012). (B) Skull anatomy of *Sinraptor dongi* (modified from Tanke and Currie 1998). (C) Skeletal reconstruction of *Sinraptor dongi* based on the preserved material (modified from Paul 2010). aof, antorbital fenestra; ltf, laterotemporal fenestra; mfe, maxillary fenestra; o, orbit; pne, pneumatic excavation in the maxilla; po, postorbital; tsl, toothstrike lesion indicated by black stippling. Silhouettes by Gregory S. Paul (*Yangchuanosaurus zigongensis*) and Scott Hartman (all others). [Colour online.]

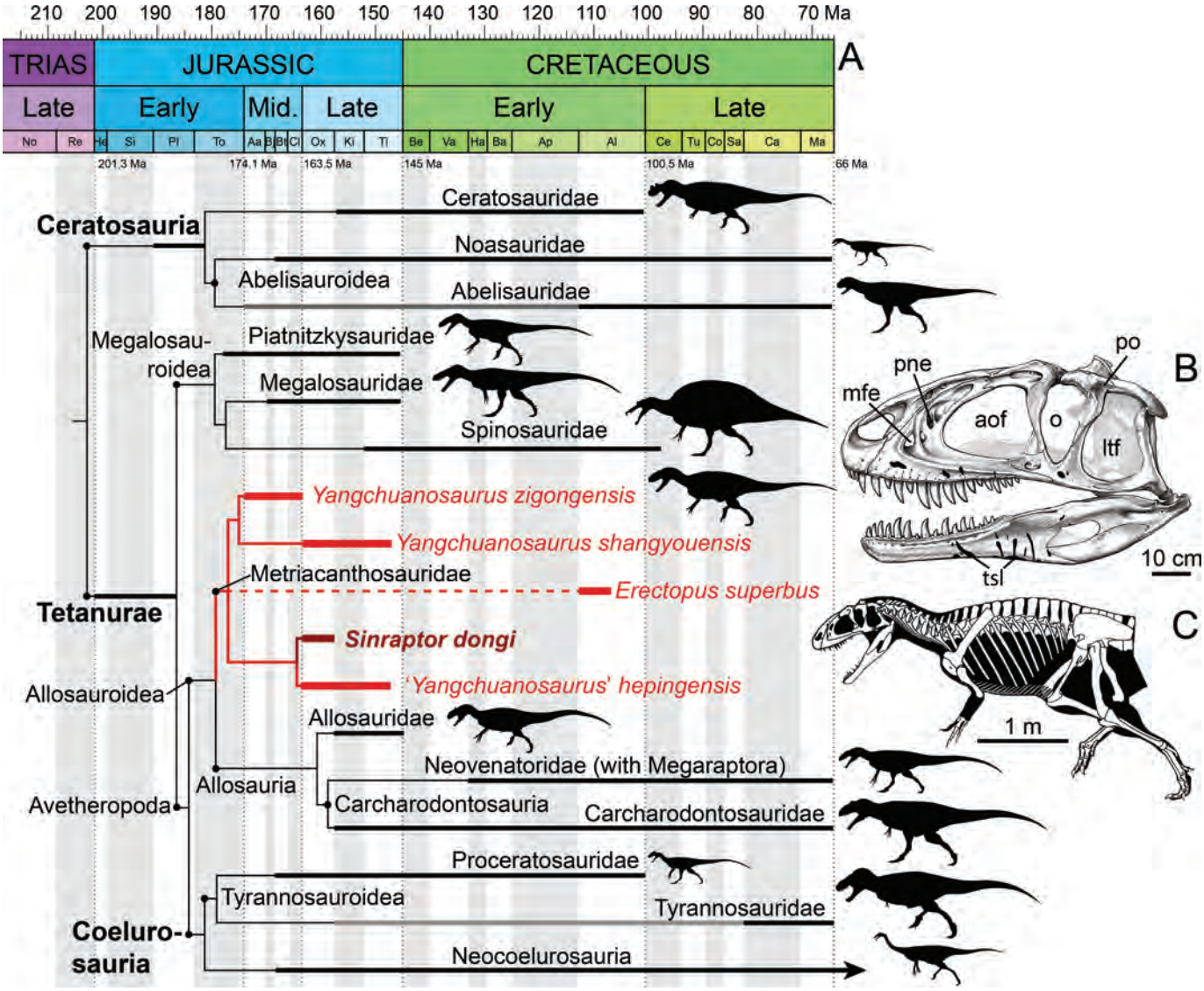

Choiniere et al. 2014*b*), and *Shishugounykus inexpectus* Qin et al., 2019. Stratigraphically, the Shishugou Formation correlates with the upper Callovian or lower Oxfordian to the upper Oxfordian, an assessment based on $^{40}Ar/^{39}Ar$ radiometric ages (Eberth et al. 2010; Choiniere et al. 2014*b*). However, because definite radiometric ages are not yet available for the underlying Xishanyao Formation or its lateral equivalents, it is possible that the Shishugou Formation is entirely Oxfordian.

Sinraptor dongi is one of the best-known members of the "family-level" clade Metriacanthosauridae, a Laurasian radiation of allosauroid theropods closely related to *Allosaurus* and extending from the Middle Jurassic to the Early Cretaceous of Europe and Asia (Fig. 2A; Currie and Zhao 1993; Carrano et al. 2012). *Sinraptor dongi* is currently known from a nearly complete skull (Figs. 1B, 1C, 2B) and a partial skeleton missing the tail and several bones of the forearm (Fig. 2C). The material was discovered by Haijun Wang in September 1987, 25 km northeast of Jiangjunmiao, Junggar Basin, Xinjiang Province. The skeleton was unearthed by a team of Chinese and Canadian paleontologists in 1987 and 1988 during the Sino-Canadian expedition known as the "Dinosaur Project" (Dong et al. 1988; Currie 1991; Dong 1993). *Sinraptor dongi* is characterized by a postorbital horn; an enlarged lateral temporal fenestra; and a highly pneumatized internal naris, maxilla, and postpalatine (Fig. 2B; Carrano et al. 2012; Currie and Zhao 1993).

Whereas the cranial and postcranial material of *Sinraptor dongi* has received a comprehensive description from Currie and Zhao (1993), the dentition morphology, surprisingly, has been little described, with information on the mesial dentition, crown ornamentation, carinae, and denticle morphology being omitted. Nonetheless, the teeth of this taxon are particularly well preserved, and most of them are still positioned in their alveoli (Fig. 1A). The scarcity of information available on the dentition of *Sinraptor*, and on metriacanthosaurids in general, led several au-

Table 1. Crown-based measurements taken of the dentition of *Sinraptor dongi* (IVPP 10600).

Position	CBL	CBW	CH	AL	CBR[a]	CHR[a]	MCL	MCW	MCR[a]	MDE
lpm4	?	?	~30	?	?	?	?	?	?	?
rpm1	13.53	18.35	?	?	1.3562	?	?	?	?	?
rpm2	13.47	19.14	?	?	1.4209	?	?	?	?	?
rpm3	16.87	17.53	?	?	1.0391	?	?	?	?	?
rpm4	20.28	12.26	?	?	0.6045	?	?	?	?	?
rmx3	24.39	12.3	59.44	59.5	0.5043	2.4371	21.43	10.27	0.4792	–4.7
rmx4	26.63	10.14	63.43	65.47	0.3808	2.3819	22.47	9.9	0.4406	–2.4
rmx6	26.74	10.22	60.07	63.48	0.3822	2.2464	22.75	9.3	0.4088	–5.25
rmx7	26.83	8.88	55.94	53.21	0.331	2.085	21.63	8.43	0.3897	–3
rmx9	24.12	9.3	?	?	0.3856	?	?	?	?	?
rmx11	18.81	7.93	?	?	0.4216	?	?	?	?	?
rmx13	14.76	6.68	21.62	20.15	0.4526	1.4648	12.46	5.52	0.443	?
rmx14	12.86	4.91	?	?	0.3818	?	?	?	?	?
rdt8	21.13	8.23	37.01	38.6	0.3895	1.7515	17.12	8.35	0.4877	0
ldt, mesial	15.33	10.2	32.29	33.33	0.6654	2.1063	15.53	8.66	0.5576	0
ldt, mesial	17.08	11.36	38	37.18	0.6651	2.2248	15.43	9.69	0.628	–2.8
rdt, mesial	18.58	11.06	>38,54	>39,27	0.5953	?	17.68	9.19	0.5198	–3.05
rdt, lateral	19.89	10.54	39.97	41.04	0.5299	2.0096	17.6	8.86	0.5034	–4.4
ldt, lateral	19	9.6	40.55	40.05	0.5053	2.1342	16.49	9.03	0.5476	0
ldt, lateral	19.58	9.48	38.42	38.97	0.4842	1.9622	17.13	8.62	0.5032	0
Position	**TUD**	**MA**	**MC**	**MB**	**DA**	**DC**	**DB**	**MAVG[a]**	**DAVG[a]**	**DSDI[a]**
lpm4	?	?	?	?	9.5	9.7	?	?	?	?
rpm1	?	?	?	?	?	?	?	?	?	?
rpm2	?	?	?	15	?	?	17	?	?	?
rpm3	?	?	?	?	?	?	?	?	?	?
rpm4	?	?	?	?	?	?	?	?	?	?
rmx3	2–3	9.375	11	21.66	?	10	20.83	14.01	15.415	1.1
rmx4	3	9	10	18.75	9.5	10	15	12.58	11.5	1
rmx6	2	10	11	17.5	8.75	10	20	12.83	12.91	1.1
rmx7	2	11	12	13.75	11.66	11.5	16.875	12.25	13.34	1.0435
rmx9	?	?	13.75	21.25	?	?	22.5	17.5	22.5	?
rmx11	?	?	15	?	?	?	?	15	?	?
rmx13	0	?	?	?	15	15	20	?	16.66	?
rmx14	?	?	?	?	?	15.83	?	?	15.85	?
rdt8	3	12	11	21.25	10	11.5	17.5	14.75	13	0.9565
ldt, mesial	0	13	12.5	15	11	11	?	13.5	11	1.1364
ldt, mesial	0	12.5	12	17.5	11	11	16	14	12.66	1.0909
rdt, mesial	0	?	11.25	18	10	11	16.5	14.625	12.5	1.0227
rdt, lateral	3	11.25	11.5	18	11	11	16	13.58	12.66	1.0455
ldt, lateral	3	11.25	11.5	16.66	9.5	10.5	18	13.14	12.66	1.0952
ldt, lateral	2–3	12	12.5	17.5	11	11.5	17	14	13.16	1.087

Note: AL, apical length; CBL, crown base length; CBR, crown base ratio; CBW, crown base width; CH, crown height; CHR, crown height ratio; DA, distoapical denticle density; DAVG, average distal denticle density; DB, distobasal denticle density; DC, distocentral denticle density; DSDI, denticle size density index; IVPP, Institute for Vertebrate Paleontology and Paleoanthropology, Beijing, China; ldt, isolated left dentary tooth; lpm, left premaxillary tooth; MA, mesioapical denticle density; MAVG, average mesial denticle density; MB, mesiobasal denticle density; MC, mesiocentral denticle density; MCL, mid-crown length; MCR, mid-crown ratio; MCW, mid-crown width; MDE, mesiobasal denticle extension; rdt, right dentary tooth; rmx, right maxillary tooth; rpm, right premaxillary tooth; TUD, transverse undulation density.
[a]Ratio variables.

thors (e.g., Han et al. 2011; Xu and Clark 2008) to tentatively assign isolated theropod teeth from the Shishugou Formation either to more inclusive clades (i.e., Tetanurae, Tyrannosauroidea) or to metriacanthosaurids.

This work aims to (*i*) provide a thorough description of the dental morphology of *Sinraptor dongi*, with the goal of facilitating the comparison of isolated theropod teeth and their assignment to this taxon; (*ii*) compare the dentition of *Sinraptor* with that of other theropods using cladistic, multivariate, discriminant, and cluster analyses; and (*iii*) investigate feeding ecologies in *Sinraptor* on the basis of dental morphology. Examination of the enamel and dentin microstructure, the microwear pattern of the crown, and the tooth replacement rate and pattern in *Sinraptor* is beyond the scope of this study. Because dentition can be used to reconstruct ecology and trophic position, this work will ultimately help sort out how the different-sized theropods from the Shishugou Formation divided the carnivorous ecomorphospace.

Materials and methods

Comparative method and terminology

The dental material of the holotype of *Sinraptor dongi* (Institute for Vertebrate Paleontology and Paleoanthropology, Beijing, China (IVPP) 10600) was examined first hand with the use of a digital microscope, AM411T-Dino-Lite Pro. Because tooth-bearing bones from the left side of the skull are currently embedded in foam on a mounted skull, we also used photographs of these specimens (taken just after they had been prepared) to describe the hidden side of the left dentition. Fourteen crown-based measurements (i.e., crown base length (CBL), crown base width (CBW), crown height (CH), apical length (AL), mid-crown length (MCL), mid-crown width (MCW), mesiobasal denticles extent (MDE), transverse undulation density (TUD), mesiobasal denticle density (MB), mesiocentral denticle density (MC), mesioapical denticle density (MA), distobasal denticle density (DB), distocentral denticle density (DC), and distoapical denticle density (DA); Table 1)

were taken with digital calipers on the best-preserved and fully accessible teeth (i.e., teeth not embedded in hard foam) following the methodology detailed by Hendrickx et al. (2015*c*, 2020). The dental anatomy of *Sinraptor dongi* was described using the nomenclature and modus operandi provided by Hendrickx et al. (2015*c*). The dentition of *Sinraptor* was compared with that of theropods with large-sized (CH > 30 mm) ziphodont teeth, including Allosauroidea, Ceratosauria, Dilophosauridae, Megalosauroidea, and Tyrannosauroidea. First-hand examination of specimens of > 70 species of non-maniraptoriform neotheropods (Supplementary Data[1]) residing in 35 scientific collections from Argentina, Canada, China, France, Germany, Italy, Portugal, Qatar, South Africa, Switzerland, the United Kingdom, and the United States formed the basis for comparison. The terminologies of Smith and Dodson (2003) and Hendrickx et al. (2015*c*) were used for anatomical orientation, whereas the morphometric and anatomical terms and abbreviations follow those defined and illustrated by Smith et al. (2005) and Hendrickx et al. (2015*c*). We followed the terminology of Hendrickx et al. (2015*c*) for cross-section types, which differentiates salinon-shaped, J-shaped, U-shaped, and D-shaped cross-sectional outlines in mesial teeth. A salinon-shaped cross section has both mesial and distal carinae facing linguomesially and linguodistally, respectively, and the labial and lingual surfaces are convex and biconcave, respectively (Hendrickx et al. 2015*c*, fig. 5R). In contrast, the J-shaped cross section corresponds to a comma-shaped outline in which the labial surface is convex, the lingual surface is sigmoid, and the mesial carina faces mesiolingually (Hendrickx et al. 2015*c*, fig. 5T). A D-shaped cross section, in which mesial and distal carinae face linguomesially and linguodistally, respectively, has wide mesiodistally convex labial and lingual surfaces (Hendrickx et al. 2015*c*, figs. 5P–5Q). It should not be confused with the U-shaped cross section, in which both carinae face lingually and there is a strongly convex labial surface and a weakly concave, convex, or biconvex mesiodistally short lingual surface (Hendrickx et al. 2015*c*, figs. 5N–5O). The nomenclature proposed by Hendrickx and Mateus (2014*b*) is used for theropod maxillae.

Cladistic and multivariate analyses

Apomorphic dental character states in *Sinraptor dongi* were identified by performing a phylogenetic analysis on a slightly revised version of the dentition-based data matrix created by Hendrickx and Mateus (2014*a*) and updated by Young et al. (2019) and Hendrickx et al. (2019, 2020). The metriacanthosaurids *Yangchuanosaurus shangyouensis* and "*Yangchuanosaurus*" *hepingensis*, as well as two character states related to enamel thickness and tooth replacement rate (characters 141 and 142), were added to the Hendrickx et al. (2020) data set so that the resulting data matrix includes 148 characters (Supplementary Data[1]) scored across 107 species. These taxa are phylogenetically bracketed between the early saurischian *Herrerasaurus ischigualastensis* (Sereno and Novas 1992, 1994) and the avialan *Archaeopteryx lithographica* (Meyer 1861; Howgate 1984; Rauhut 2014; Rauhut et al. 2018; Supplementary Data[1]). The distribution of apomorphic dental character states was visualized on a fully topologically constrained tree (sensu Hendrickx et al. 2020) using WinClada 1.00.08 (Nixon 2002) on the basis of a Nexus file, with the data matrix and the phylogenetic tree, both created with Mesquite 3.2 (Maddison and Maddison 2017). The tree topology is congruent with the results recovered by Müller et al. (2018), fifth phylogenetic analysis (which uses the data matrix of Langer et al. 2017) for non-neotheropod saurischians, Ezcurra (2017) for non-averostran neotheropods, Rauhut and Carrano (2016) and Wang et al. (2017) for Ceratosauria, Carrano et al. (2012) and Rauhut et al. (2012, 2016) for non-coelurosaurian tetanurans, Brusatte and Carr (2016) for Tyrannosauroidea, and Cau et al. (2017) on the basis of the data set of Brusatte et al. (2014) for neocoelurosaurs (i.e., Compsognathidae + Maniraptoriformes; sensu Hendrickx et al. 2019).

Two methods were followed to visualize which taxa are close to *Sinraptor dongi* in terms of qualitative dental character states: First, a cladistic analysis was performed on the data matrix of dentition-based characters (Supplementary Data[1]), as well as on a reduced data matrix restricted to tooth-based characters using the software TNT (Goloboff et al. 2008). The tooth-based data matrix comprises 91 characters (characters 38–122 and 143–148) scored across 102 dentulous taxa (Supplementary Data[1]), with the basally branching saurischian *Herrerasaurus* (Sereno and Novas 1994) as the outgroup taxon to root the tree. The search strategy of each analysis used a combination of the tree-search algorithms Wagner trees, TBR branch swapping, sectorial searches, Ratchet (perturbation phase stopped after 20 substitutions), and Tree Fusing (five rounds), until 100 hits of the same minimum tree length were achieved. The best trees obtained were subjected to a final round of TBR branch swapping (the TNT command used is "xmult = hits 100 rss fuse 5 ratchet 20" followed by the "bb" command). Bremer support, absolute bootstrap frequency, and difference in bootstrap frequency (also known as the GC (for "Group present/Contradicted") bootstrap frequency; Goloboff et al. 2003) were calculated for the strict consensus tree of the most parsimonious trees (MPTs). Second, a principal coordinate analysis (PCoA) was conducted on the distance matrix generated from the dentition-based data matrix using the software R and the R package Claddis (Lloyd 2016). The morphospace occupation of *Sinraptor* and other theropods was mapped onto the first two principal coordinate axes capturing the largest amount of variation.

Morphometric analyses

To know whether the premaxillary, maxillary, dentary, mesial, and lateral crowns of *Sinraptor* can be distinguished from one another, and whether *Sinraptor* teeth can be discriminated from those of other theropods on the basis of quantitative data, a discriminant function analysis (DFA) was conducted using the data set compiled by Hendrickx et al. (2015*b*) and recently supplemented by Young et al. (2019) and Hendrickx et al. (2020). The DFA is a statistical procedure that classifies unknown teeth into a certain group such as a positional entity along the tooth row or a genus-level taxon (Moore 2013; see Williamson and Brusatte (2014) and Richter et al. (2013) for further information on this technique). To check whether separation of the morphotypes is justified (Gerke and Wings 2016), we also performed a principal component analysis (PCA). This multivariate technique extracts a set of measurements taken on a sample of teeth into a smaller set of axes (typically two) that describe the primary variability among the specimens, allowing the teeth of each taxon to be plotted in morphospace to see whether there is separation or overlap (Williamson and Brusatte 2014). The data set of Hendrickx et al. (2020) includes 15 crown-based measurements (i.e., CBL, CBW, CH, AL, crown base ratio (CBR), crown height ratio (CHR), MCL, MCW, mid-crown ratio (MCR), mesial serrated carina length (MSL), number of flutes on the labial surface (LAF), number of flutes on the lingual surface (LIF), crown angle (CA), mesial denticle length (MDL), distal denticle length (DDL); n.b., Young et al. (2019) and Hendrickx et al. (2020) incorrectly use the abbreviations DCL and DDC for DDL) taken from 1335 teeth belonging to 78 non-avian theropod taxa (75 species and three indeterminate family-level taxa; Supplementary Data[1]). Both DFA and PCA were performed on the data set of Hendrickx et al. (2020) restricted to the measurements taken by the first author (C.H.) and to taxa with large (CH > 20 mm) ziphodont crowns. The final data set comprises 400 teeth belonging to 46 large theropod taxa. A second analysis

[1]Supplementary data are available with the article through the journal Web site at http://nrcresearchpress.com/doi/suppl/10.1139/cjes-2019-0231.

was conducted on the same data set this time restricted to allosauroid taxa (Supplementary Data[1]). Both DFA and PCA were run in Past3 version 3.19 (Hammer et al. 2001) using the linear discriminant analysis (LDA) and principal component (PCA) functions, respectively, following the methodology detailed by Hendrickx et al. (2020). DFA and PCA were conducted at the species level, first by using an arbitrary value of 100 denticles per 5 mm for unserrated carinae, then by considering the absence of denticles as unknown data.

We additionally performed a cluster analysis to visualize which genus-level theropods group with *Sinraptor* on a drendrogram on the basis of tooth crown measurements. The cluster analysis was conducted in Past3 on the data set restricted to taxa with large (CH > 20 mm) ziphodont crowns using a classical–hierarchal clustering, Euclidean distances for the Similarity Index, and a Paired Group algorithm, as well as a Neighbour Joining clustering, rooting the tree with the final branch in both classical–hierarchal and Neighbour Joining clustering.

Results

Cladistic and multivariate analyses

The distribution of dental character states on the resultant tree reveals that no dental apomorphies diagnose *Sinraptor dongi*, whereas a single dental apomorphy diagnoses the clade comprising *Sinraptor dongi* and *Yangchuanosaurus hepingensis* (Fig. 3A; Supplementary Data[1]). Two and three dentition-based synapomorphies, respectively, diagnose the clades Metriacanthosauridae and Allosauria, whereas nine dental character states diagnose allosauroid theropods (Fig. 3A; Supplementary Data[1]). The cladistic analysis conducted on the dentition-based data matrix yielded 100 MPTs whose strict consensus tree is relatively well resolved and includes one major and several minor polytomies (Supplementary Data[1]). *Sinraptor dongi* is recovered as the sister taxon of "*Yangchuanosaurus*" *hepingensis* in a dentition-based clade composed of non-abelisauroid ceratosaurs, tyrannosaurids, *Yangchuanosaurus shangyouensis*, and *Allosaurus* (Fig. 3B). Conversely, the cladistic analysis performed on the tooth-based data matrix yielded 100 MPTs and a poorly resolved strict consensus tree that includes a large polytomy comprising more than 30 taxa (consistency index = 0.173; retention index = 0.407; length = 920; Supplementary Data[1]). However, *Sinraptor dongi* is recovered in a partially resolved clade gathering most pantyrannosaurian tyrannosauroids, forming a polytomy with *Allosaurus*, *Neovenator*, "*Yangchuanosaurus*" *hepingensis*, and *Yangchuanosaurus shangyouensis* (Fig. 3C).

The two-dimensional (2D) morphospace based on the first two principal coordinate axes and generated from the PCoA performed on the dentition-based data matrix reveals that *Sinraptor dongi* occupies the same region of morphospace as do most ziphodont theropods (i.e., non-averostran theropods, abelisaurids, megalosaurids, neovenatorids, carcharodontosaurids, tyrannosauroids, and dromaeosaurids; Supplementary Data[1]). "*Yangchuanosaurus*" *hepingensis*, followed by *Afrovenator*, *Ceratosaurus*, *Fukuiraptor*, and *Yangchuanosaurus shangyouensis*, are the closest taxa to *Sinraptor dongi* in the PCoA plot. The first two PCoA axes, however, only capture an extremely weak amount of variation (4.21% and 2.37%), and this result should therefore be considered cautiously.

Morphometric analysis

The results of the DFA conducted on the data set of crown-based measurements reveal that the premaxillary, maxillary, and dentary teeth of *Sinraptor dongi* occupy different regions of morphospace (first principal component (PC1), 84.01%; second principal component (PC2), 15.99%; Fig. 4A; Supplementary Data[1]). The results of the PCA conducted on the same data set show that the range of morphospace occupation is the highest and lowest for maxillary and premaxillary teeth, respectively (Supplementary Data[1]). The PCA plot also reveals that the morphospace occupations of dentary and maxillary teeth slightly overlap. Right maxillary tooth (rmx) 11, rmx14, and the isolated left lateral dentary crowns indeed share relatively similar sizes and proportions. Although the morphospace occupation of premaxillary and dentary teeth is non-overlapping, one isolated left mesial dentary tooth and the fourth right premaxillary tooth are next to each other in the PCA plot. Teeth from the mesial and lateral dentition of *Sinraptor dongi* do not overlap, and the range of morphospace occupation is greatest among the lateral teeth (Supplementary Data[1]).

The 2D plots resulting from the DFA and PCA conducted on the data set with ziphodont theropod crowns of >2 cm show that the teeth of *Sinraptor dongi* occupy the same region of the morphospace as do those of ceratosaurids, abelisaurids, megalosaurids, allosaurids, and tyrannosaurids (Supplementary Data[1]). Despite considerable overlap in the morphospace occupation of *Sinraptor*, *Abelisaurus*, *Allosaurus*, *Ceratosaurus*, and *Duriavenator* (Supplementary Data[1]), eight out of 11 teeth were correctly identified as belonging to *Sinraptor* in the DFA, with the remaining teeth being ascribed to *Allosaurus* (two teeth) and *Abelisaurus* (one tooth; Supplementary Data[1]). This result is obtained with or without considering unserrated carinae as having 100 denticles/5 mm. The success rate of the DFA is slightly higher, however, when a high number of denticles for unserrated carinae is taken into account (PC1, 48.78%; PC2, 24.92%; success rate, 59.83%), rather than considering the absence of denticles as unknown data (PC1, 43.64%; PC2, 31.72%; success rate, 58.79%). Among allosauroid theropods, the DFA could successfully discriminate 80% of teeth at the species level. Ten out of 11 teeth were correctly identified as belonging to *Sinraptor*, the remaining tooth being classified as a crown of an *Allosaurus* tooth (PC1, 64.56%; PC2, 20.48%; Supplementary Data[1]). The 2D plot shows that the morphospace occupation of *Sinraptor* teeth fully overlaps that of *Allosaurus* and only partially that of *Mapusaurus* (Fig. 4B). The range of occupation of *Sinraptor* teeth is particularly limited compared with those of *Acrocanthosaurus*, *Allosaurus*, *Carcharodontosaurus*, and *Giganotosaurus* (Fig. 4B).

Results of the cluster analysis performed on the data set restricted to large-sized teeth show that *Sinraptor* crowns are retrieved in the same morphoclade as those of non-noasaurid ceratosaurs, megalosauroids, allosauroids, and tyrannosauroids using both hierarchal and Neighbour joining clustering (Fig. 5; Supplementary Data[1]). Most *Sinraptor* teeth were recovered in two separate morphoclades, in which they cluster with ceratosaurid teeth (Fig. 5).

Systematic paleontology

Dinosauria Owen, 1842
Saurischia Seeley, 1887
Theropoda Marsh, 1881
Tetanurae Gauthier, 1986
Avetheropoda Paul, 1988
Allosauroidea (Marsh, 1878)
Metriacanthosauridae Paul, 1988

Sinraptor dongi Currie and Zhao, 1993

MATERIAL: IVPP 10600, a nearly complete skull and partial skeleton (Figs. 2B, 2C).

TYPE LOCALITY AND HORIZON: Jiangjunmiao, Junggar Basin, Xinjiang Uygur Autonomous Region, China; upper beds of the Shishugou Formation; Oxfordian, Late Jurassic (Currie and Zhao 1993; Carrano et al. 2012). The upper beds of the Shishugou Formation in Jiangjunmiao are likely correlative with those from the Wucaiwan locality of Xinjiang (Choiniere et al. 2014*a*).

State of preservation

A detailed account of the preservation of the dentition of *Sinraptor dongi* is provided in the Supplementary Data[1].

Fig. 3. Distribution of allosauroid dental character states and results of the cladistic analyses. (A) Distribution of apomorphic dentition-based character states diagnosing allosauroid clades and taxa (phylogenetic tree based on the results obtained by Carrano et al. 2012). White and black circles represent ambiguous and unambiguous dental apomorphies, respectively. (B) Strict consensus tree limited to the region of the tree with *Sinraptor dongi*, from 40 MPTs resulting from a cladistic analysis performed on a dentition-based data matrix of 148 characters coded across 107 non-avian theropod taxa. (C) Strict consensus tree limited to the region of the tree with *Sinraptor dongi*, from 100 MPTs resulting from a cladistic analysis performed on a crown-based data matrix of 91 characters scored across 102 non-avian theropod taxa. Metriacanthosaurid taxa are in red for B and C. Silhouettes by Gregory S. Paul (*Yangchuanosaurus shangyouensis*), T. Tischler (*Fukuiraptor*), and Scott Hartman (all others). [Colour online.]

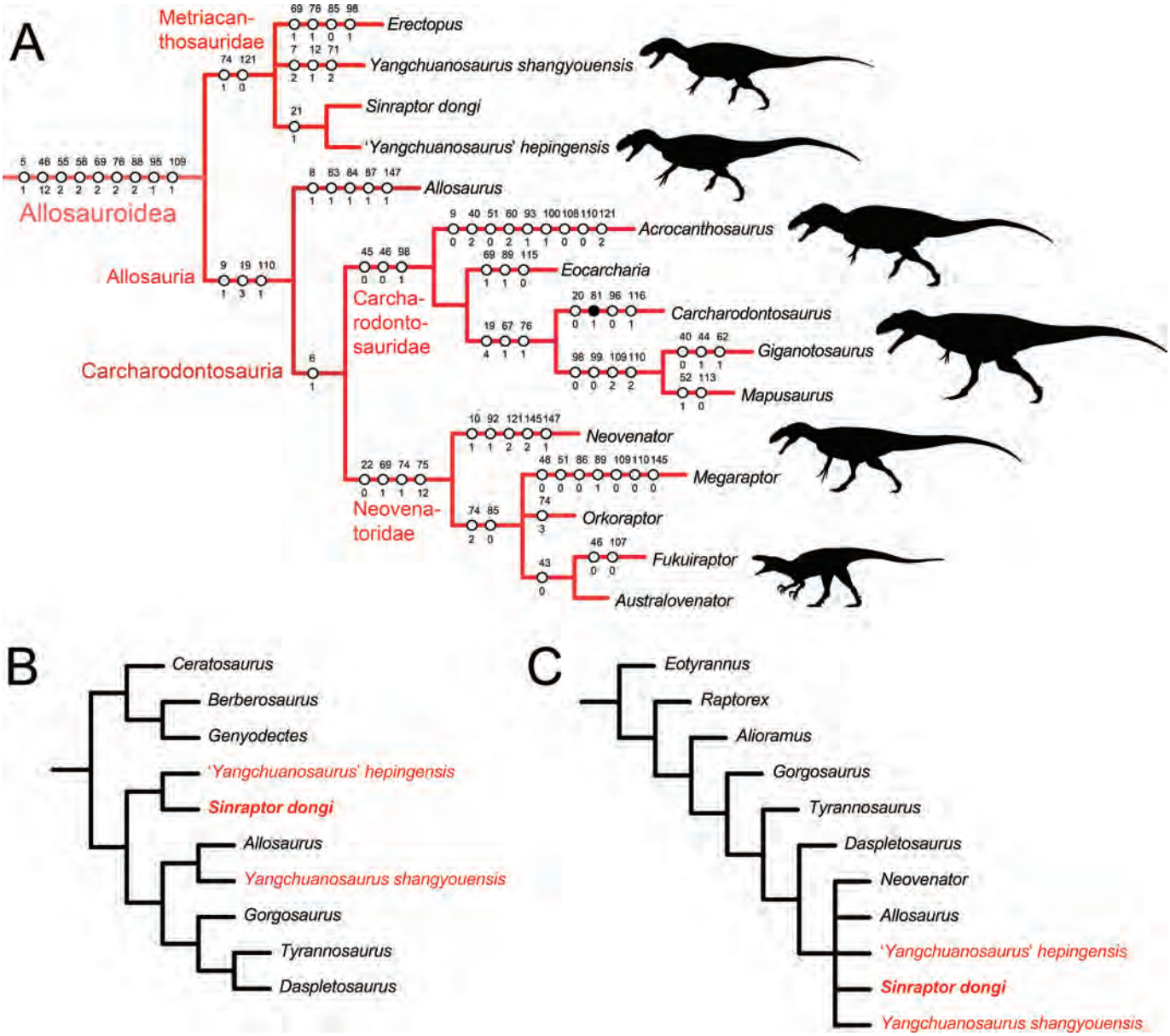

General dentition morphology

Each premaxilla of *Sinraptor dongi* bears four teeth; the left and right maxillae have 15 and 14 alveoli, respectively; and the left dentary has 16 tooth positions (Currie and Zhao 1993). The apex of a 15th crown from the second generation of teeth is visible within a minute alveolus ventral to the medial wall of the right maxilla (Supplementary Data, Fig. S2E[1]), at the level of the nutrient groove (sensu Hendrickx and Mateus 2014*a*). However, no alveolus is present distal to the 14th alveolus, at the level of the alveolar margin, ventral to the second crown generation. There are 12 alveoli in the preserved portion of the right dentary, and a total of 16 teeth was likely present on the basis of the reconstructed bone. All teeth are ziphodont, denticulated, distally curved, and without a constriction at the base of the crown. No teeth have bifurcated (or splitted) carinae.

With a CH of 63.43 in rmx4 and a CHR of 2.43 in rmx3, the tallest and most elongate crowns are found in the mesiocentral part of the maxilla, between the third and sixth alveoli in the right maxilla (Fig. 6; Table 1) and the fifth and eighth alveoli in the left maxilla. With mean CBL and CH values of 21.9 and 52.1 mm, respectively, the teeth of the maxilla are also larger, on average, than those of the premaxilla (CBL of 16 mm; CH of approximately 30 mm for rpm4; Table 1) and the dentary (CBL of 18.65 mm; CH of 37.7 mm). The premaxilla has the thickest crowns (mean CBW of

Fig. 4. Results of the discriminant analysis (DFA). (A) Plot resulting from the DFA performed on a data set of 20 teeth belonging to the right premaxilla, right maxilla, and left and right dentary of *Sinraptor dongi* (IVPP 10600; skull reconstruction of *Sinraptor* based on Currie and Zhao (1993), modified). (B) Plot resulting from the DFA performed on a data set of 114 teeth belonging to eight allosauroid taxa (*Allosaurus* silhouette by Scott Hartman). Morphospace occupation of *Sinraptor dongi* in thick black dash lines. DA, distoapical denticle density; DB, distobasal denticle density; dt, dentary teeth; MA, mesioapical denticle density; MB, mesiobasal denticle density; MDE, mesiobasal denticles extent; MDL, mesial denticle length; MSL, mesial serrated carina length; mx, maxillary teeth; pm, premaxillary teeth. [Colour online.]

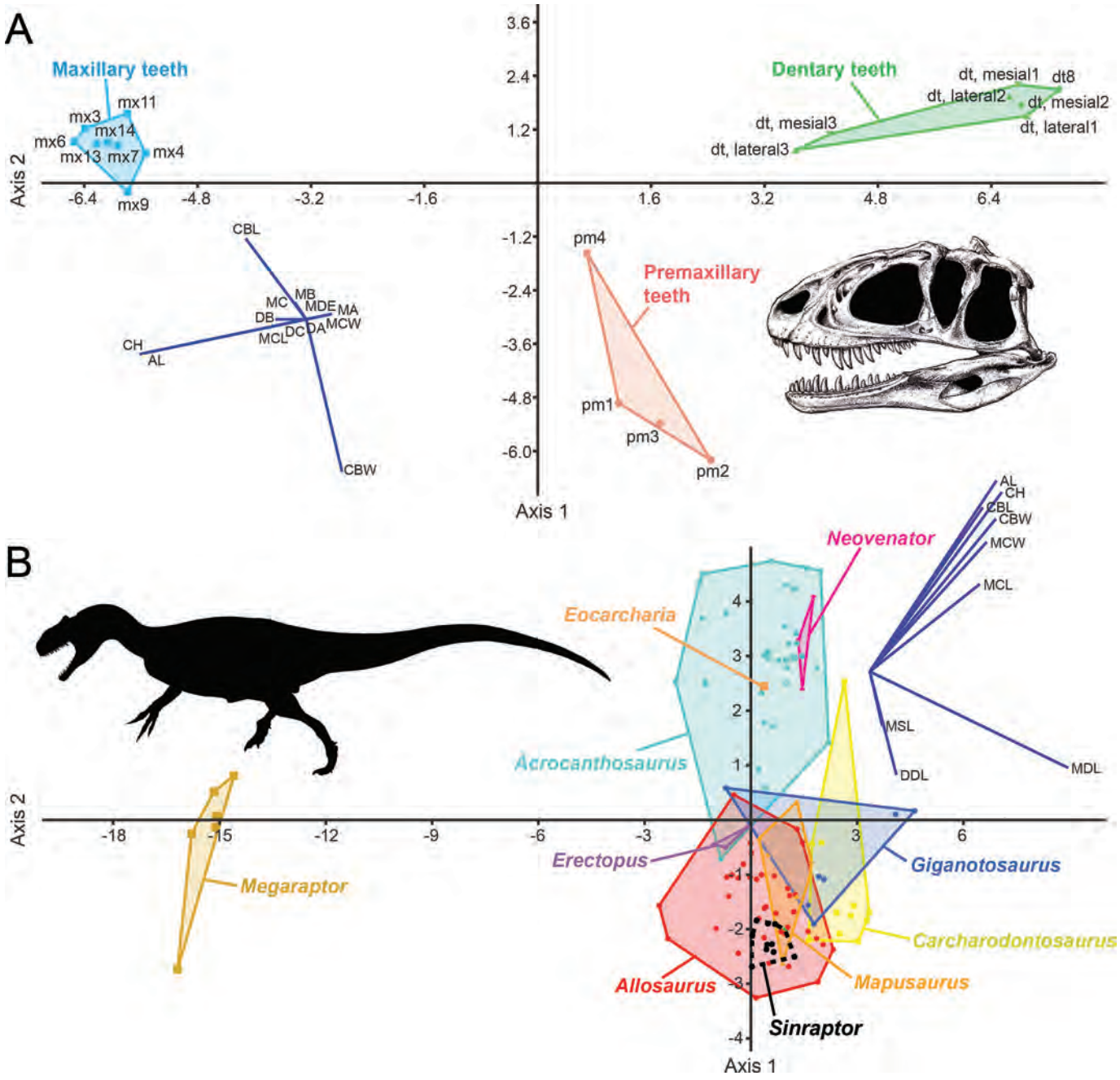

16.82 mm; CBR of 1.1), whereas the most labiolingually compressed crowns are found in the maxilla (mean CBW of 8.79 mm; CBR of 0.4; Fig. 6; Table 1) at the anteroposterior midpoint of the bone (between maxillary teeth mx4 and mx9), where the teeth are highly compressed (CBR of approximately 0.37). Unlike CBW, CBLs of the right premaxillary teeth increase from the second (13.74 mm) to the fourth (20.28 mm; Fig. 6) crowns. On the basis of the preserved teeth of the left premaxilla, the same pattern is observed in the premaxillary CH (Currie and Zhao 1993). Although CH increases up to the fourth right maxillary crown, then decreases in more distal teeth, CBL increases towards the seventh tooth (26.83 mm), whereas CBW gradually decreases from the third (17.53 mm) to the 14th crowns (4.91 mm; Table 1). If maxillary teeth become shorter distally (i.e., CHR values gradually decrease from rmx3 (2.43) to rmx13 (1.46); Table 1), the crown thickness (i.e., CBR and MCR) remains relatively constant along the rmx row, fluctuating from 0.5 (rmx3) to 0.33 (rmx7). Interestingly, if teeth are as compressed or slightly more compressed at mid-crown than at the cervix in mesial and anterior lateral teeth (CBR of approximately 0.57; MCR of approximately 0.52), it is the opposite for the

Fig. 5. Results of the cluster analysis using (A) classical–hierarchical and (B) Neighbour joining clustering. Colours of taxa represent their phylogenetic affinities: beige = non-abelisauroid Ceratosauria; yellow = Abelisauridae; light green = Spinosauridae; dark green = Piatnitzkysauridae and Megalosauridae; light red = Metriacanthosauridae; red = Allosauridae; dark red = Carcharodontosauridae; purple = Tyrannosauridae. Teeth of *Sinraptor* are in black and bold. [Colour online.]

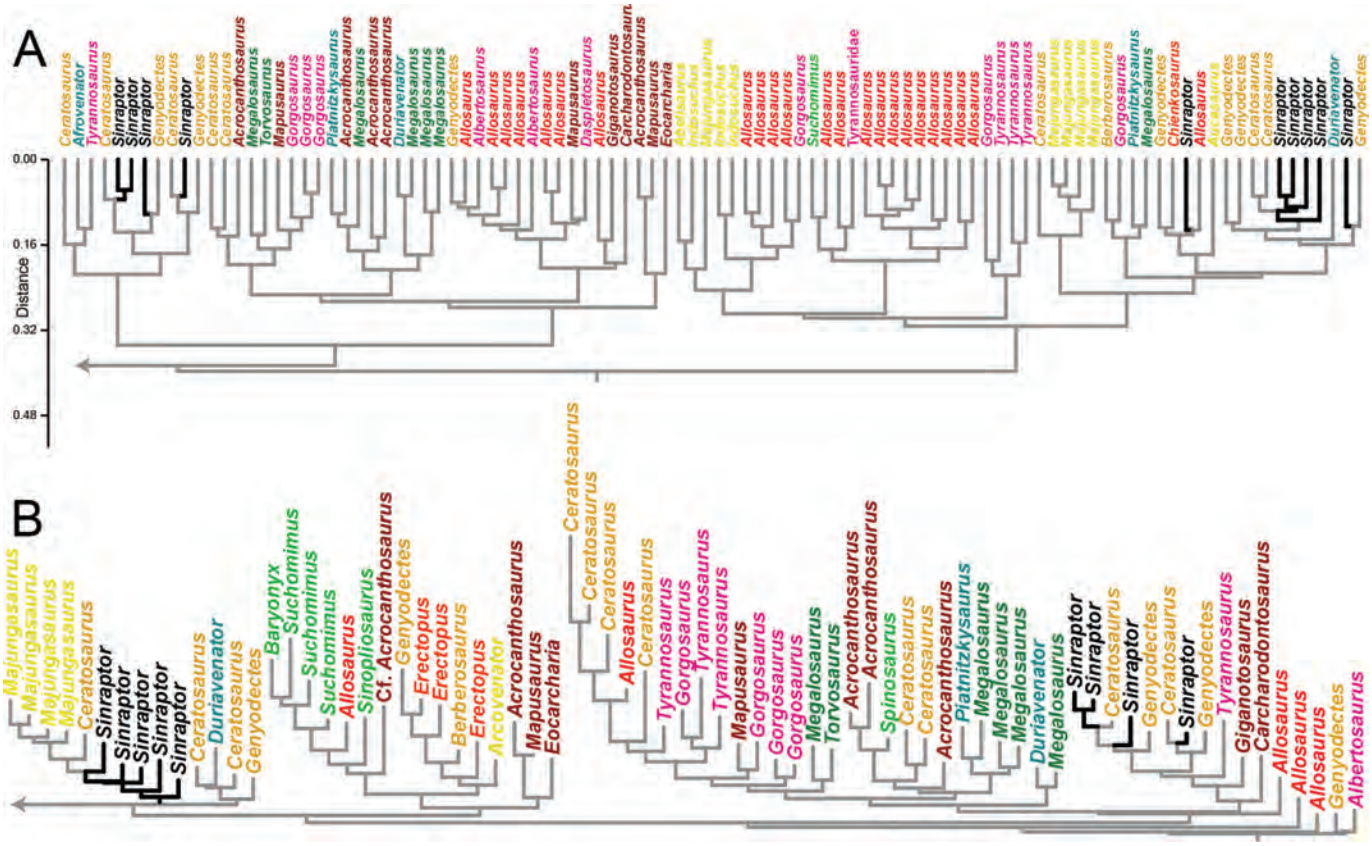

lateral dentition from the central portions of the maxilla and dentary, where teeth are significantly more compressed at the bases of the crowns (CBR of approximately 0.37; MCR of approximately 0.43). A general decrease in crown size (i.e., CBL and CH) occurs distal to rmx4 and lmx5, with the distalmost maxillary crowns being only slightly higher than long. Conversely, the numbers of mesial and distal denticles in the central parts of the carinae remain stable until rmx6 (11 denticles/5 mm). This number then gradually increases distally to reach 15–16 denticles/5 mm in both mesial and distal carinae in rmx11 to rmx14 (Fig. 6; Table 1).

Given the presence of a single preserved fully erupted tooth in the right dentary, and isolated teeth of unknown position from the left and right dentaries, no trends along the dentary tooth row can be determined for *Sinraptor dongi*. However, the distinction between the mesial and lateral teeth among the sample of isolated dentary teeth enables us to provide some information on dental trends in the dentary. On average, mesial dentary teeth are shorter, lower (mean CBL and CH of 17 and 35.14 mm, respectively), less elongate (mean CHR of 2.16), slightly thicker and less compressed (mean CBW and CBR of 10.87 mm and 0.64, respectively) than are lateral teeth (mean CBL, CBW, CH, CBR, and CBR of 19.49 mm, 9.87 mm, 39.65 mm, 0.51, and 2.03, respectively; Table 1). The right dentary tooth (rdt) 8, which is believed to be the most distal dentary tooth preserved, is the least elongate (CHR of 1.75) and the most labiolingually compressed (CBR of 0.39; Table 1). With a CBL of 21.13 mm, rdt8 is also the longest of all dentary crowns. Unlike that of the maxilla, the mesiocentral and distocentral denticle densities are relatively constant along the dentary tooth row, with MC and DC fluctuating between 10.5 and 12.5 denticles/5 mm (Table 1). Nonetheless, this tendency likely results from the fact that no teeth distal to the eighth dentary alveolus are preserved. Indeed, the distalmost dentary teeth probably had a higher number of denticles per 5 mm compared with those present in the anterior half of the dentary.

Mesial dentition

The premaxillary teeth and three isolated teeth belonging to the anterior portions of the left and right dentaries are used in describing the mesial dentition of *Sinraptor dongi* (Figs. 7 and 8). The mesial teeth are labiolingually thick, with a CBR ranging from 0.6 to 1.43. The thickest crowns are those of the first two premaxillary teeth (CBR between 1.35 and 1.42). It is possible, however, that the mesialmost dentary teeth of *Sinraptor*, which may not be preserved within the sample of isolated mesial dentary teeth, were as thick as those of the premaxilla. The mesial dentition is also moderately elongate, with a CHR ranging from 1.8 (left premaxillary tooth (lpm) 4) to 2.2 (isolated left dentary teeth). Mesial teeth are only weakly curved, with the distal profile of the crown being straight to slightly convex in lingual view.

The first two premaxillary teeth are slightly recurved lingually to linguodistally, whereas the more distal premaxillary crowns, as well as the preserved mesial dentary teeth, curve distally. The mesial and distal carinae of the mesial dentition are denticulated for all of the CH and to a certain distance onto the root base, significantly below the cervical line on the labial and lingual surfaces of the crown (Figs. 8P–8T). The distal carina is weakly bowed, with the apex of the convexity being labially directed in distal view. The distal carina is also slightly deflected labially along the basal two-thirds of the crown, being almost centrally positioned in the apical third of the crown. Each mesial tooth shows a

Fig. 6. Crown-based measurements across the premaxilla, maxilla, and dentary of *Sinraptor dongi* (IVPP 10600). (A) Millimetres. (B) Ratio. (C) Denticles/5 mm. CBL, crown base length; CBR, crown base ratio; CBW, crown base width; CH, crown height; CHR, crown height ratio; DC, distocentral denticle density (per 5 mm); dt, dentary tooth; la, lateral dentary tooth; MC, mesiocentral denticle density (per 5 mm); MCR, mid-crown ratio; me, mesial dentary tooth; mx, maxillary tooth; pm, premaxillary tooth. [Colour online.]

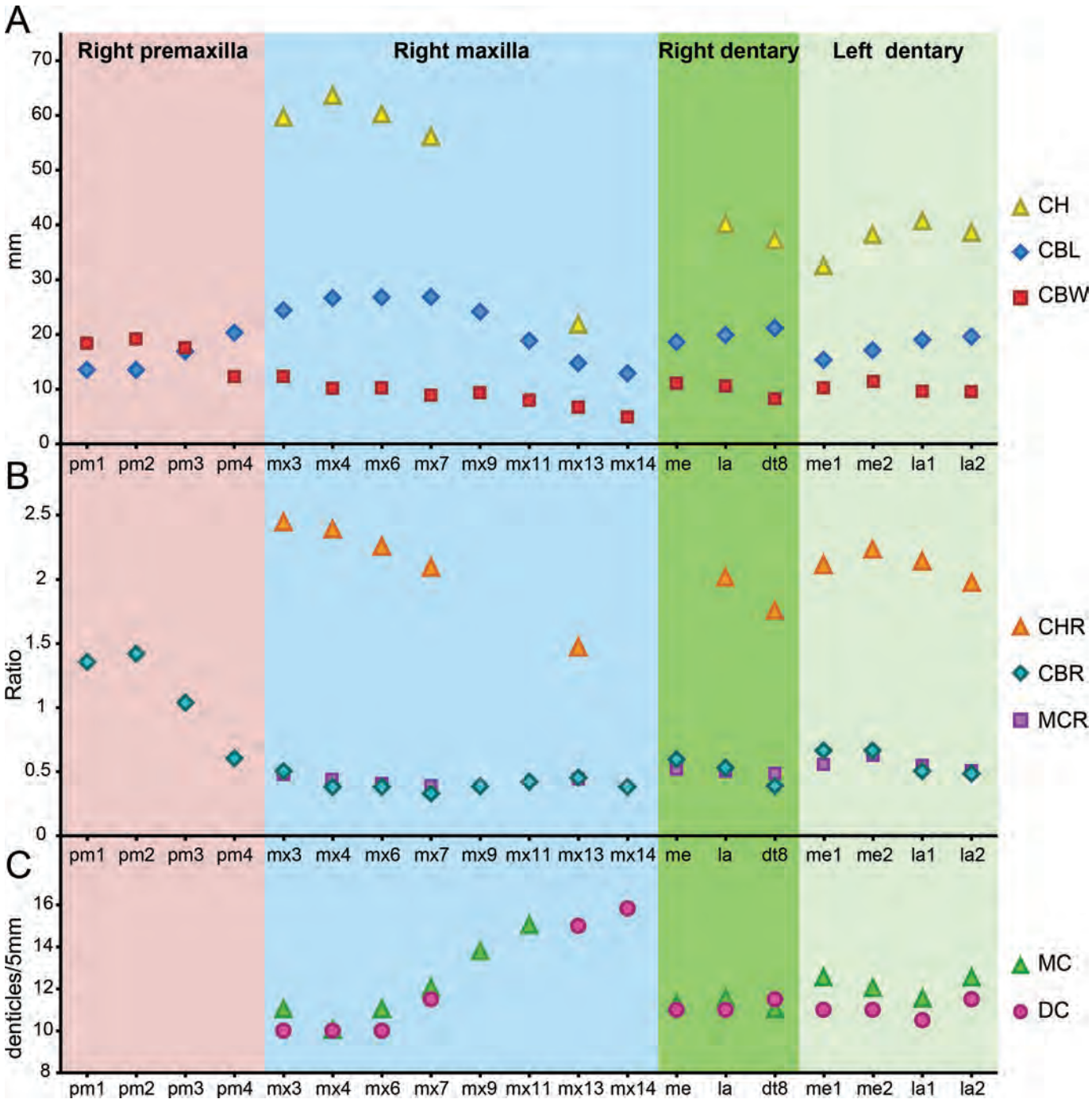

strongly linguomesially deflected mesial carina in mesial view, so that the mesial carina is strongly deflected lingually at the crown base (Figs. 7B, 7C, 7E, 8E, 8J, 8S). On the basis of the crown cross-sectional outline and photos of the left premaxillary dentition in lingual view (Fig. 7E), the mesial carinae are particularly deflected linguomesially in pm1 and pm2. The carinae cross the tips of the crowns in lpm3 and most likely all other mesial teeth, but are worn off with the crown apices in the mesial dentary teeth. The distal carina extends more basally than the mesial carina, and the cervical line, easily visible on the crown, angles slightly basodistally, at an angle of 10° to 15° in lateral view.

A longitudinal groove adjacent to the mesial carina, on the lingual surface of the crown, characterizes all mesial teeth of *Sinraptor*. This groove runs along the entire CH and is closer to the mesial carina basally. Such grooves are clearly present in lpm3 and lpm4 (Figs. 7B, 7D, 7E) and all mesial dentary teeth (Fig. 8T), but they seem to be shallow or absent in the first two premaxillary teeth (Figs. 7B, 7E). The lingual surfaces are also mesiodistally

Fig. 7. Premaxillary dentition of *Sinraptor dongi* (IVPP 10600; photos taken before the left premaxilla was mounted using foam). First to fourth left premaxillary teeth in (A) labial, (B) lingual, and (C) apical–palatal views, with close-up on the premaxillary teeth in (D) apicolingual and (E) mesiolingual views. 2nd uet, second-generation unerupted tooth; cos, concave surface; mca, mesial carina; pm, premaxillary tooth; sps, spalled surface. Scale bars equal 2 cm. [Colour online.]

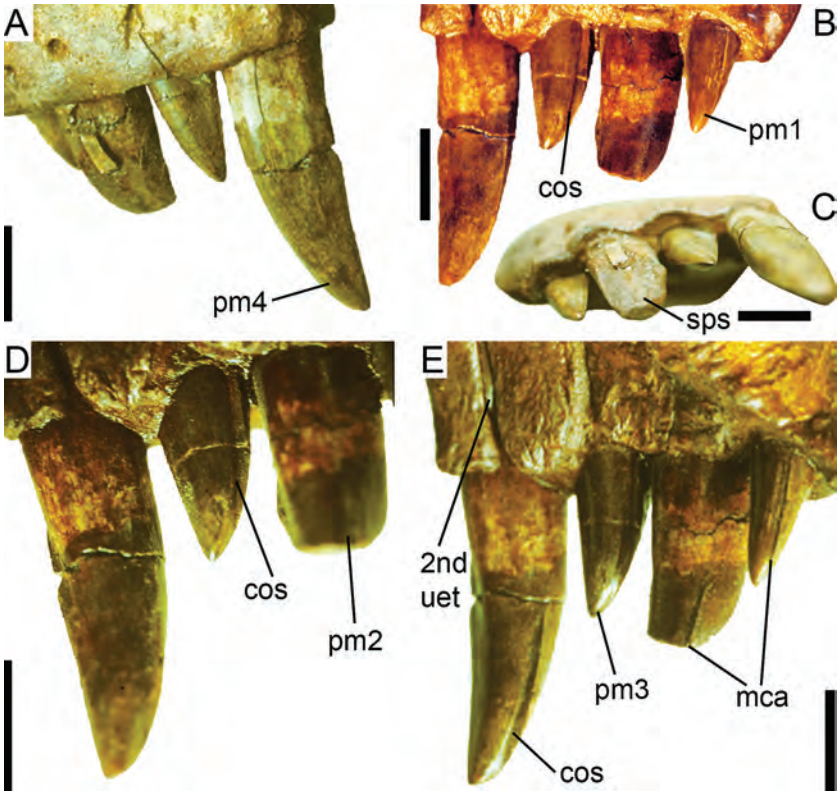

concave marginal to the distal carinae in rpm2 and rpm3 (Fig. 8D), lpm2 to lpm4 (Currie and Zhao (1993), fig. 2D; Figs. 7B, 7D, 7E), and one mesial dentary tooth (Fig. 8H). However, this linguodistal concavity is more pronounced in rpm3 than in rpm2. A similar concavity is also visible on the labial surface of lpm3, adjacent to the distal carina (Fig. 8A). The concavity appears to be mesiodistally wider and more pronounced basally in this partially erupted crown, fading away at the apex. Although weak, similar concavities are present in rpm2 and rpm3 on the basis of the cross-sectional outlines of these two crowns. A distal concavity is absent, however, on the labial surface of each of the mesial dentary teeth. Finally, the labial surface is flat to very weakly concave marginal to the mesial carina in rpm2. However, a labiomesial concavity adjacent to the carina is absent in all other mesial teeth. Given the presence of a mesial and sometimes distal concavity marginal to each carina of the lingual surface of the crown, the cross-sectional outline of mesial teeth varies between salinon and J-shaped. An asymmetrical salinon-shaped outline characterizes the crown base of rpm3 (Figs. 8B, 8D), whereas a J-shaped outline better describes the crown base cross section of mesial dentary teeth. The cross-sectional outline of the root base of rpm2 can be described as labiolingually elongated D-shaped, but it is unknown whether the cross section of the crown had the same shape at the cervix. The lingual surface is strongly mesiodistally convex in rpm2, whereas rpm3 has a weaker convexity in apical view (Fig. 8D). On the basis of the cross-sectional outlines of the preserved teeth from the right premaxilla, the long axis is linguodistally oriented in all crowns but is particularly oriented lingually in rpm1, and distally in rpm4 (Fig. 8D). The morphologies of mesial and distal denticles, interdenticular sulci, crown features (e.g., transverse undulations, spalled surfaces), and enamel surface textures visible in mesial teeth will be described in the next sections.

The roots of mesial teeth, well preserved and fully visible in the isolated dentary teeth, are long and are 1.5 to 2 times the CHs. The root tapers apically and shows weakly convex mesial and distal profiles in lateral view, with the apices of the mesial and distal convexities at two-fifths and one-third of the root height, respectively. The long axis of the root is roughly vertical in the first two-thirds of the height, and then it gently curves distally in the apical third in lateral view. In mesial and distal views, the root is straight and slightly linguobasally inclined from the long axis of the crown, and it becomes labiolingually compressed basally. In lateral view, the labial profile of the tooth is convex all along its height, with the apex being at the same level as the cervix or directly basal to it. Conversely, the lingual profile of the root is either weakly convex or flat in lateral view. The root is hollow and elliptic in cross section at one-third of its height. A deep and well-defined resorption pit is visible on the lingual surface in two mesial dentary teeth (Fig. 8G). The resorption pit extends along the apical two-thirds of the root. It is bounded by the labial wall of the root all along its height and by the mesial and distal walls along its basal half. The resorption pit hosted the second-generation tooth in one mesial dentary tooth and two generations of teeth in another. In the latter, the track of the crown of the second-generation tooth is visible directly basal to the resorption pit. This well-delimited depression, which gives the cross section of the root a figure-eight outline directly apical to the resorption pit, extends along the mesial and distal walls of the root marginal to the mesial and distal margins of the pit. Such a deep resorption pit is absent in a third mesial dentary tooth. The resorption pit instead corresponds to a shallow depression in the central part of the lingual side of the root (Fig. 8E). The pit extends along the apical three-quarters of the root, and its lingual surface is mesiodistally undulating in its basal part.

Fig. 8. Mesial dentition of *Sinraptor dongi* (IVPP 10600). (A) Second to fourth left premaxillary teeth in labial view. (B) Cross-sectional outline of the third right premaxillary tooth at the crown base. First to fourth right premaxillary tooth in (C) lingual and (D) apical views. First isolated right mesial dentary tooth in (E) lingual and (F) labial views. Second isolated right mesial dentary tooth in (G) lingual, (H) distal, (I) labial, (J) mesial, (K) apical, and (L) basal views, with close-up on (M) the enamel surface texture, (N) interdenticular sulci and distocentral denticles, and (O) mesiocentral denticles in lateral views. Close-up on the crown in (P) lingual, (Q) distal, (R) labial, (S) mesial, and (T) linguomesial views. Apex of isolated left mesial dentary crown in (U) lingual and (V) mesial views. ce, cervix; cos, concave surface; dca, distal carina; ent, enamel surface texture; ert, erupting tooth; ids, interdenticular sulci; lgr, longitudinal groove; mca, mesial carina; pm, premaxillary tooth; rep, resorption pit; sps, spalled surface; tun, transverse undulation. Scale bars equal 2 cm (A–J), 1 cm (K–L and U–V), 5 mm (M), and 2 mm (N and O). [Colour online.]

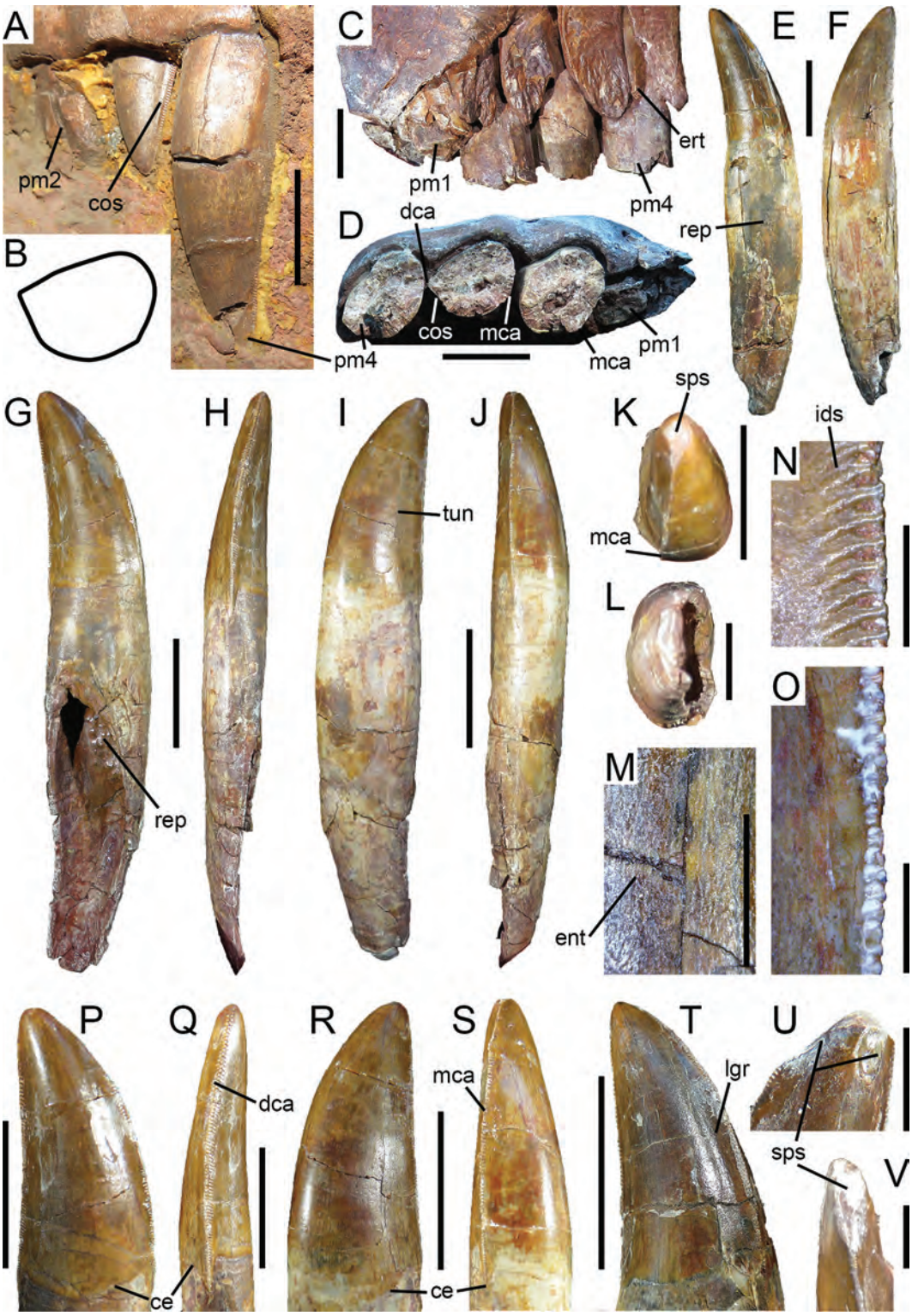

Lateral dentition

The lateral crowns of *Sinraptor dongi* differ from those of the mesial dentition mainly in labiolingual compression, the positions of the mesial carinae, and the cross-sectional outlines. As in the mesial dentition, the denticulated mesial and distal carinae of the lateral teeth extend all along the crowns, from the crown apices to cervixes, at certain distances onto the basal portions of the roots. The cervical line is also slightly to strongly inclined basally towards the distal margin of the crown in lateral view (Figs. 9B, 9C, 9K, 10A, 10C, 10K, 10M). Likewise, the lateral crowns are only slightly curved distally, so that the distal profile of each is straight to weakly concave, and the crown apex lies at the same level as the basalmost point on the distal margin in labial view (Figs. 9A, 9B, 10A, 10K). The most anterior maxillary teeth (lmx1 and rmx3) appear to be the most strongly curved of the lateral dentition, and their crown apices are slightly to strongly deflected apically from the distal margin of the crown base (Figs. 9A, 9C). As in the mesial teeth, the distal carina is weakly to strongly deflected labially and bowed in distal view, with the apex of the convexity directed labially. This is particularly the case in the first four maxillary teeth, in which the distal carinae lie at almost the same levels as the labiodistal surfaces of the crowns (Figs. 9D, 9F). The distal carina remains slightly labially deflected in each maxillary tooth; however, the apical portion of rdt9 (Fig. 9M) and at least one loose lateral tooth possibly belonging to a distal portion of the left dentary, have carinae centrally positioned on the distal profiles of the crowns. The mesial carinae of the crowns from most of the lateral dentition also spiral linguomesially towards the basal parts of the crowns, as in mesial teeth. However, these twists are less pronounced than in the mesial dentition, so that the basal part of the mesial carina is only weakly deflected lingually (Figs. 9H, 10D, 10E, 10N, 10O). The mesial carina, however, remains centrally positioned on the mesial surface of the crown in the partially erupted rdt9?, as well as in rmx9 and all more distal maxillary teeth (Fig. 9L).

A concave surface adjacent to the distal carina is present on the lingual surface of several mesial maxillary and mid-dentary crowns (e.g., rmx3–rmx7, rdt8?; Fig. 9I). This concavity is restricted to the basal half of the linguodistal surface in each of the crowns of rmx3 and rmx4 but extends for almost the entire CH in each of rmx6 and rmx7 (Fig. 9I). Similar concavities marginal to the distal carinae can also be seen on the labial surface of some maxillary teeth (e.g., rmx3, lmx5, rdt8?). However, this depression is restricted to the basal third of the crown. Instead, the basolabial surfaces of the crowns next to the distal carinae are flat in other maxillary crowns and are typically distolingually oriented in the teeth more distal than rmx3. Unlike in mesial teeth, there is no longitudinal groove marginal to the mesial carina in any lateral crowns. Likewise, the central portions of the labial and lingual surfaces of the maxillary crown are roughly flat and extend basally into shallow and mesiodistally concave depressions (Figs. 9D, 9F, 9I, 9K). Such labial depressions are clearly visible in all fully erupted maxillary and dentary teeth (Fig. 10Q; Supplementary Data[1]). However, a lingual depression is present on each crown other than those of the distalmost maxillary teeth, in which it does not extend beyond the root (Fig. 10N). The flattened labial and lingual surfaces typically extend along the basal two-thirds of the crown and are restricted to the central portion of the tooth surface, a few millimeters away from the mesial and distal carinae. The cross-sectional outline of each lateral tooth is lenticular at mid-crown in *Sinraptor dongi* because of the presence of angular mesial and distal profiles due to the carinae (Fig. 9G). However, the outline of a lateral tooth is slightly more labiolingually compressed in the distal half of the crown and less pointed in the mesial half (Fig. 9J). The cross-sectional outlines are figure-8-shaped at the levels of the cervix in most lateral teeth. Those from the distalmost portion of the maxilla are reniform in outline because of the labial depressions extending onto the bases of the crowns.

The general root morphology of most lateral teeth follows that of a mesial tooth with a shallow and poorly delimited resorption pit. The root weakly tapers apically in lateral and distal views, and has a convex mesial profile. The main axis is inclined from that of the crown in distal views. The distal profile can be slightly convex, concave, or sigmoid. Two isolated lateral teeth, one from the dentary and the other from the distalmost part of the dentition (Supplementary Data, Fig. S2[1]), have a deep and well-delimited resorption pit extending onto the apical third to apical two-thirds of the lingual side of the root. The apical tip of the pit, which corresponds to a deep depression delimited by labiolingually tall walls, is situated at mid-width of the root. Both the mesial and the distal profile of this pit are convex and follow that of the crown tip of the second generation of tooth. The resorption pits of the other lateral crowns consist of shallow and mesiodistally convex depressions along the central portions of the whole roots. A similar, yet shallower, depression is present on the labial surface to the root, giving an figure-8-shaped cross-sectional outline to the root at mid-height (Fig. 10F).

Denticles

The denticle densities are highest at the bases of the mesial and distal carinae. Conversely, the number of apical denticles is slightly lower than or similar to those from mid-CH (Table 1). Both mesial and distal denticles diminish in apicobasal length basally and apically, but this decrease in denticle size occurs over a much longer distance at the base of the crown. Denticles indeed diminish in size a few millimetres (i.e., 2–3 mm) away from the crown apex and along the basal third of the crown. Likewise, denticles tend to increase slightly in size apically within the apical two-thirds of the crown, especially on the distal carina. Only two teeth (rdt8 and one isolated mesial left dentary tooth) show a slightly higher number of apical denticles on the mesial carina, a tendency that is not observed in the distal carina (Table 1). The increase or decrease in mesial and distal denticle size is gradual, and no sporadic variation in denticle size occurs. The denticle densities range from 16 to 22.5 denticles/5 mm in the basalmost parts of the mesial and distal carinae, from 10 to 16 at mid-crown, and from 8.75 to 15 at the apex (Table 1). The largest crowns have 10 to 11 and 11 to 12 denticles/5 mm in the central parts of the distal and mesial carinae, respectively. With a denticle size density index close to one and fluctuating between 0.95 and 1.14 (Table 1), no discrepancy between mesial and distal denticles is observed in *Sinraptor dongi*.

Denticles of mesial and lateral teeth generally share the same morphology. They are perpendicular to or weakly distally inclined from the external margin of the crown (Figs. 8N, 8O, 10I, 10J) and are present all along the carinae. Most distal denticles are horizontally subrectangular, moderately to strongly mesiodistally elongate (i.e., DHR sensu Hendrickx et al. (2015*c*) of 1.3–1.5), and typically mesiodistally longer than those on the mesial carina (Figs. 8N, 8O, 10I, 10J). Only the most basal and most apical distal denticles are subquadrangular and, more rarely, vertically subrectangular. Conversely, the mesial denticles are subquadrangular in the central and apical two-third portions of the crown, with the basal and apical denticles being more vertically subrectangular in outline. The labial and lingual surfaces of the mesial and distal denticles are apicobasally convex and are labially and lingually inclined in apical views, respectively, so that a transverse section through the denticles would be subtriangular. The external margins of both mesial and distal denticles are parabolic in outline and symmetrically to asymmetrically convex, and they are never hooked apically in lateral view. When asymmetrically convex, the apex of the convexity is apically positioned. The external margins of some distal denticles are also semicircular, and we did not observe bilobate denticles along the carinae. The interden-

Fig. 9. Maxillary and dentary dentition of *Sinraptor dongi* (IVPP 10600). (A) Left maxillary dentition in labial view. (B–I) Right maxillary dentition, with close-up on (B) eighth to 14th teeth, and third to seventh teeth in (B and C) labial and (D) apical views. (E) Apex of the fourth tooth in labial view. (F) First to 13th teeth in apicolingual view. (G) Ninth to 12th teeth in apical view and 13th to 14th teeth in mesioapical view. (H) Third and fourth teeth in mesial view. (I) Sixth and seventh teeth in linguodistal view. (J) Cross-sectional outline of the 11th right maxillary crown at mid-crown. Right mid-dentary dentition, with close-up on (K) putative seventh to ninth teeth in lingual view and putative eighth tooth in (L) mesial and (M) distal views. cos, concave surface; dca, distal carina; dt, dentary tooth; lid, lingual depression; mca, mesial carina; mx, maxillary tooth; sps, spalled surface. Scale bars equal 5 cm (A–C and F), 2 cm (D, G, K, and M), and 1 cm (E, I, and L). [Colour online.]

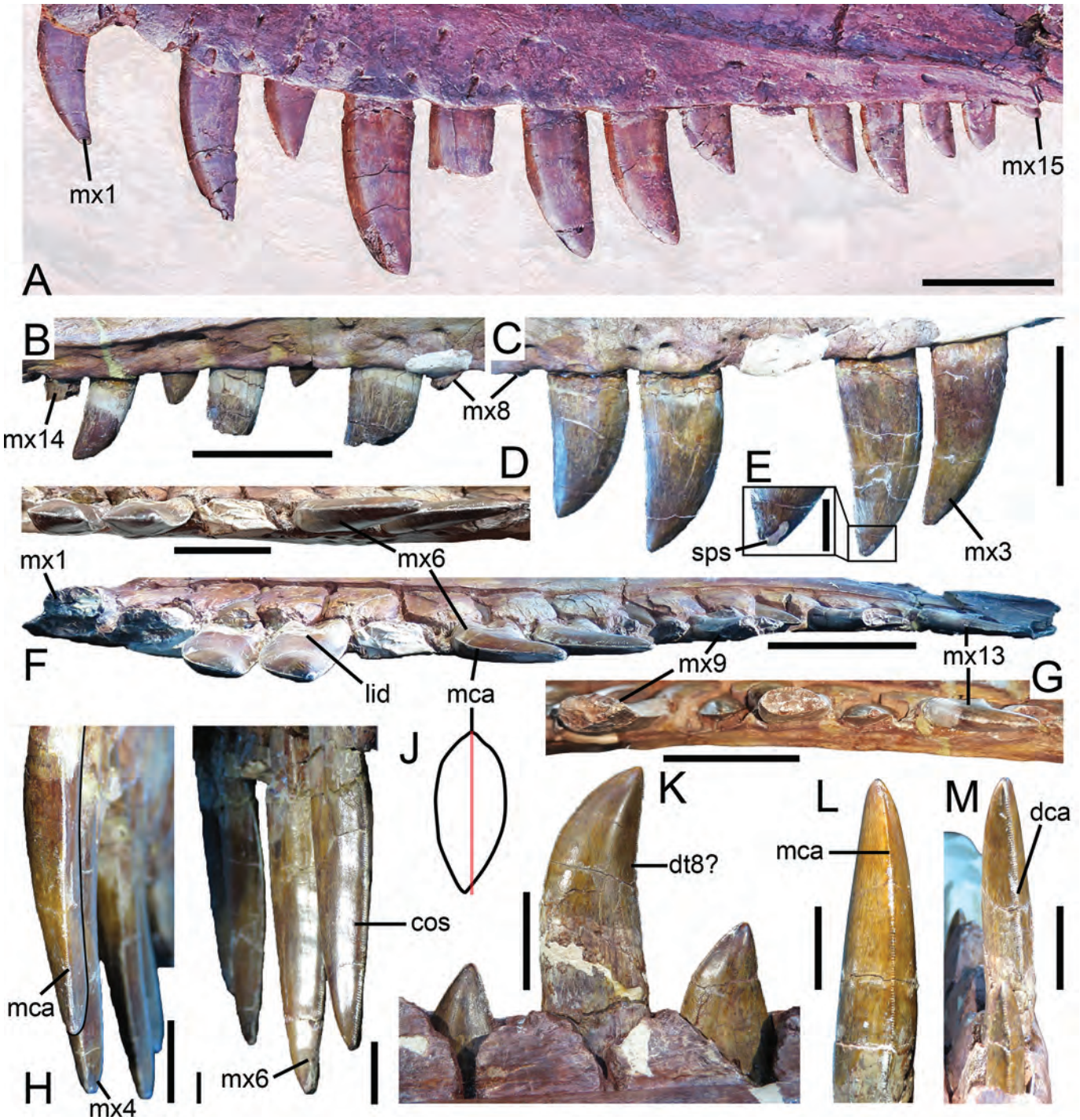

ticular space is wide between distal denticles and narrow between mesial denticles. Interdenticular sulci are present in all mesial and lateral teeth, being best developed on the labial surface of the crown, between the distocentral denticles, where they are curved basally (Figs. 8N, 10H, 10P). They are also present, but short to moderately developed, in mesiocentral and mesioapical denticles, where they either extend perpendicular to the mesial margin of the crown or are weakly oriented basally (Fig. 10J).

Crown ornamentation and enamel surface texture

The enamel surface texture of both mesial and lateral crowns is irregular and non-oriented (Figs. 8M, 10G). Transverse undulations

Fig. 10. Lateral dentition of *Sinraptor dongi* (IVPP 10600). Isolated left lateral dentary tooth in (A and I) labial, (B) distal, (C and J) lingual, (D) mesial, (E) apical, and (F) basal views, with close-up on (I) distocentral and (J) mesiocentral denticles. Isolated right lateral dentary tooth in (G, H, and K) lingual, (L) distal, (M) labial, (N) apical, and (O) mesial views, with close-up on (G) enamel surface texture, and (H) interdenticular sulci between distal denticles. (P) Weak marginal undulations adjacent to the distal carina in the eighth? right dentary tooth in labiobasal view. (Q) Transverse undulations on the seventh left maxillary tooth in apicolabial view (courtesy of Roger Benson). ce, cervix; dca, distal carina; ent, enamel surface texture; ids, interdenticular sulci; mca, mesial carina; mun, marginal undulation; tun, transverse undulation. Scale bars equal 2 cm (A–F and K–O), 1 cm (P–Q), and 1 mm (G–J). [Colour online.]

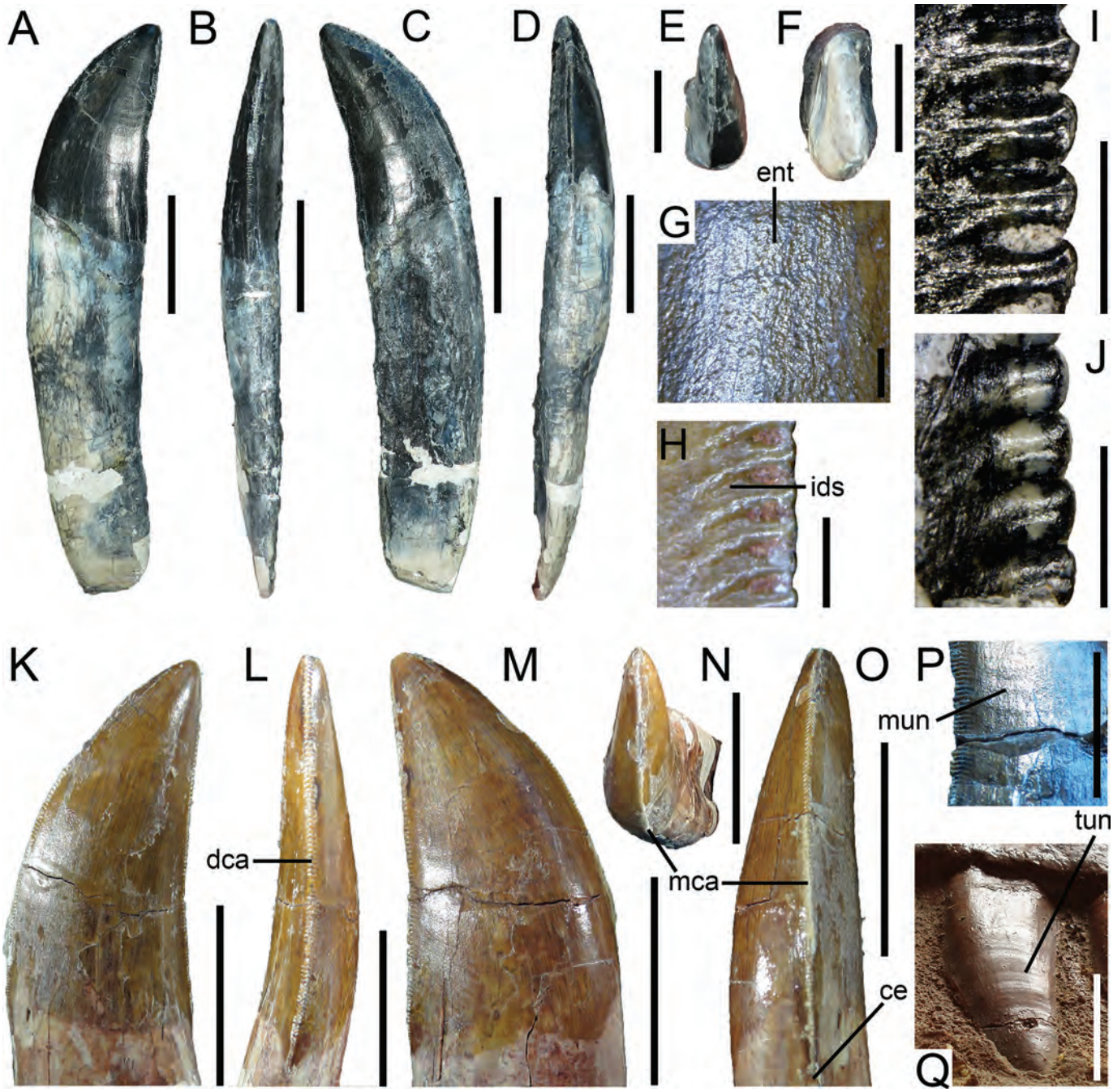

are present on most lateral crowns, but they appear to be absent in the mesial dentition and in the distalmost maxillary teeth. These band-like wrinkles extend mesiodistally from the mesial to the distal margin of the crown. Typically, they are numerous and closely packed, especially on the labial side of the tooth (Fig. 10Q). They are present on both the labial and the lingual sides of rmx3 and rmx4 and are restricted to the lingual surfaces in rmx6 and rmx7. Conversely, they appear to be restricted to the labial surface in each lateral dentary crown. Transverse undulations are densely packed (2–3 undulations per 5 mm) and typically tenuous; they are easily visible in apicolabial view on the labial surfaces of lmx5 to lmx7, one lateral dentary tooth, and on the lingual surfaces of lmx6 and lmx7. Marginal undulations are also present in rdt8?, corresponding to three poorly defined mesiodistally elongate wrinkles adjacent to the distal carina and restricted to the labiocentral portion of the crown (Fig. 10P). These undulations are likely homologous to the transverse undulations, sharing the same morphology and density and differing only in the fact that

they do not extend onto the central and mesial portions of the crown.

The enamel undulations, the longitudinal grooves adjacent to the mesial carina, the concavities marginal to the carinae, and the labial and (or) lingual depressions present at the crown base are the only crown ornamentations. Flutes, longitudinal ridges, and basal striations cannot be seen in the dentition of *Sinraptor dongi*. The crown apices, however, have spalled surfaces in various positions and with different degrees of extension. In mesial teeth, spalled surfaces are absent in lpm3 and lpm4 and are restricted to the apical portions of the crown tip in two mesial dentary teeth (Fig. 8K). The crown apex of the third mesial dentary tooth is strongly worn, with the spalled surfaces extending onto the mesial, linguodistal, and distal portions of the crown (Figs. 8U, 8V). The mesial spalled surface is basally inclined; it is the most extensive and extends on the apical quarter of the crown. The linguodistal spalled surface consists of an apicobasally elongate and elliptical surface restricted to a small portion of the distal half of the crown apex (Figs. 8U, 8V). Spalled surfaces can also be seen on the crown apices of rmx3, rmx4, rmx6, and rmx7. They are limited to the most apical parts of the tips and are present on both labial and lingual surfaces in rmx3, rmx6, and rmx7. However, in rmx4, the spalled surface is restricted to the labial side of the crown, is strongly basomesially elongated, and is reniform in outline (Fig. 9E). A photo from several complete to nearly complete isolated teeth recovered with the skull material of *Sinraptor dongi* (IVPP V10600; Supplementary Data, Fig. S2[1]) shows the presence of extensive spalled surfaces in most of the shortest crowns. The apices of these teeth, which are here interpreted as being from the distalmost portion of the dentition, are also missing. Spalled surfaces, whose long axes are oriented diagonally, extend basodistally along the apical two-thirds of the crowns and almost reach the cervix in one of them (Supplementary Data, Fig. S2[1]).

Discussion

Comparative anatomy

Results of the cladistic, multivariate, and cluster analyses, which were based on qualitative and quantitative data, show that the general dentition and crown morphology of *Sinraptor dongi* are relatively similar to those of other non-maniraptoriform averostrans such as ceratosaurids, megalosaurids, allosaurids, metriacanthosaurids, neovenatorids, and tyrannosaurids (Figs. 3B, 3C, 4B). All these large-bodied carnivorous theropods share ziphodont or pachydont dentition comprising distally curved denticulated crowns and mesial teeth that are labiolingually thicker than those from lateral dentitions (Hendrickx et al. 2015*a*, 2015*c*, 2019). Ziphodont and pachydont theropods also have larger maxillary teeth (compared with premaxillary and dentary dentitions), in which the longest and highest crowns are typically found in the anterior portion of the maxillary tooth row (Smith 2005, 2007, Hendrickx et al. 2015*b*). Nevertheless, results of the DFA indicate that the crowns of *Sinraptor* can be discriminated easily from those of other theropods included in the analyses, suggesting that the dentition of *Sinraptor* might in fact be as diagnostic as those of *Spinosaurus*, *Tyrannosaurus*, and *Troodon* solely on the basis of quantitative data. However, this result should be considered cautiously given that the sample of *Sinraptor* teeth from our data set is relatively limited (11 teeth only) and that closely related species from Metriacanthosauridae are poorly represented.

Excluding other metriacanthosaurid theropods, whose dentition will be described comprehensively in another contribution, the dentition of *Sinraptor dongi* is strikingly similar to that of *Allosaurus* in terms of both discrete characters and quantitative data (Figs. 3B, 3C, 4B). Results of the DFA indeed indicate that some teeth of *Sinraptor* can be easily confused with those of *Allosaurus* on the basis of tooth crown measurements. *Sinraptor* and *Allosaurus* have many dental features in common, including (*i*) denticulated mesial and distal carinae extending to the cervix and (or) onto the root base in both mesial and lateral teeth; (*ii*) strongly lingually twisted mesial carinae facing linguomesially in mesial teeth; (*iii*) concave surfaces adjacent to the mesial and distal carinae, resulting in a salinon- or J-shaped cross-sectional outline of the crown base in mesial teeth; (*iv*) labially deflected distal carinae; (*v*) closely packed transverse and marginal undulations; (*vi*) wide interdenticular spaces; (*vii*) well-developed interdenticular sulci; and (*viii*) irregular surface textures of the enamel (Hendrickx et al. 2019; Fig. 11). Such a combination of dental features is absent in carcharodontosaurians and all other non-allosauroid archosaurs with ziphodont teeth (C.Hendrickx, personal observation). In fact, the mesial and lateral tooth morphology of *Sinraptor dongi* and *Allosaurus* is almost indistinguishable. Both taxa have particularly thick mesial crowns whose mesial and distal carinae extend to the cervix. The carinae of the first two premaxillary teeth are strongly lingually deflected, and the mesial carina faces linguomesially in *Allosaurus*, giving a D-shaped cross-sectional outline to the crown base (Figs. 11E, 11G, 11H). Although the cross-sectional outlines of the first two premaxillary crowns are unknown in *Sinraptor dongi*, the section through the root base of rpm2 suggests that both carinae were also positioned on the lingual half of the tooth, with a mesial carina twisting onto the linguomesial side of the crown (Fig. 8D). The mesial teeth from more distal positions in the premaxilla and dentary, which can be referred to as "transitional teeth", also share the same morphology in *Sinraptor dongi* and *Allosaurus*. These transitional crowns are characterized by mesial carinae that twist strongly lingually, distal carinae that are deflected slightly to strongly labially, and concave surface and (or) longitudinal grooves marginal to the mesial carinae; these features convey a J-shaped outline to the crown at the cervix (Figs. 8P–8T, 11I, 11N). Finally, the lateral teeth of *Sinraptor dongi* and *Allosaurus* share slightly lingually twisted and labially deflected mesial and distal carinae in the central parts of the maxillary and dentary tooth rows, and centrally positioned mesial and distal carinae in the posterior thirds of these two tooth-bearing bones (Figs. 9D, 9E, 11Q–11W).

The dentition of *Sinraptor* differs from that of *Allosaurus* mainly in the number of premaxillary teeth and in the curvatures and thickness of the lateral teeth. *Allosaurus* is known to have had five premaxillary teeth, an apomorphy shared with *Neovenator* among Allosauroidea (Madsen 1976; Brusatte et al. 2008; Loewen 2010). Some *Allosaurus* lateral crowns are also weakly recurved, but the lateral dentition includes mainly slightly to strongly curved crowns with convex distal crown margins. Conversely, most lateral teeth have straight distal crown margins in *Sinraptor dongi*, and only those from the anteriormost part of the maxilla are significantly recurved (Figs. 9A–9C). Finally, with an average CBR of 0.65 in *Allosaurus* and 0.43 in *Sinraptor dongi*, the lateral teeth of *Allosaurus* are significantly thicker than those of *Sinraptor dongi* and other allosauroids (C.Hendrickx, personal observation). This is clearly illustrated in the results of the cluster analysis, in which the crowns of *Sinraptor* cluster with those of ceratosaurids rather than with those of allosaurids (Fig. 5). Ceratosaurid teeth are known to have particularly labiolingually compressed lateral crowns (Rauhut 2004; Hendrickx and Mateus 2014*a*), whereas allosaurids have pachydont teeth typical of tyrannosaurids (Hendrickx et al. 2019).

Interestingly, many dental features shared between *Sinraptor dongi* and *Allosaurus* are convergently present in some Abelisauridae from the Upper Cretaceous of the Southern Hemisphere. Similar to those of *Sinraptor* and *Allosaurus*, the dentition of the best-known abelisaurid, *Majungasaurus*, displays transverse and marginal undulations, well-developed interdenticular sulci, and irregular enamel surface textures (Fanti and Therrien 2007; Smith 2007; Hendrickx et al. 2020). In addition, the denticulated mesial and distal carinae extend to the bases of the roots, and mesial

Fig. 11. Dentition of *Allosaurus* sp. Isolated mesialmost tooth (lpm1–lpm2 or rdt1; UMNH VP 6145) in (A) labial, (B) mesial, (C) lingual, (D) distal, and (E) apical views. (F) Marginal undulations adjacent to the distal carina on the labial surface of a mesialmost tooth (UMNH VP 5837) in labiobasal view. (G) Cross section and (H) cross-sectional outline at the base crown of the first left premaxillary tooth (UMNH VP 9258) in apical view. Isolated mesial ("transitional") tooth (UMNH VP 5812) in (I) labial, (J) mesial, (K) lingual, (M) distal, and (N) apical views, with (L) cross-sectional outline at mid-crown (based on the cross-sectional outline of the fourth left dentary tooth of UMNH VP 6476 at mid-crown). (O) Enamel surface texture of the seventh right dentary tooth (UMNH VP 9351) in labial view. (P) Mesioapical denticles of an isolated lateral tooth (UMNH VP 7436) in lateral view. Isolated lateral tooth (UMNH VP 5841) in (Q) labial, (R) mesial, (S) lingual, (U) distal, and (V) apical views, with (T) cross-sectional outline at mid-crown (based on the cross-sectional outline of rpmx4 YPM 14554 at mid-crown). (W) Interdenticular sulci between distocentral denticles in an isolated lateral tooth (UMNH VP 6177) in lingual view. (X) Distocentral denticles of the fourth left premaxillary tooth (UMNH VP 6499) in labial view. cos, concave surface; dca, distal carina; ids, interdenticular sulci; idsp, interdenticular space; lid, lingual depression; lgr, longitudinal groove; mca, mesial carina; mun, marginal undulation; tun, transverse undulation. Scale bars equal 1 cm (A–G, I–N, and Q–V), 5 mm (N), and 1 mm (O–P and W–X). [Colour online.]

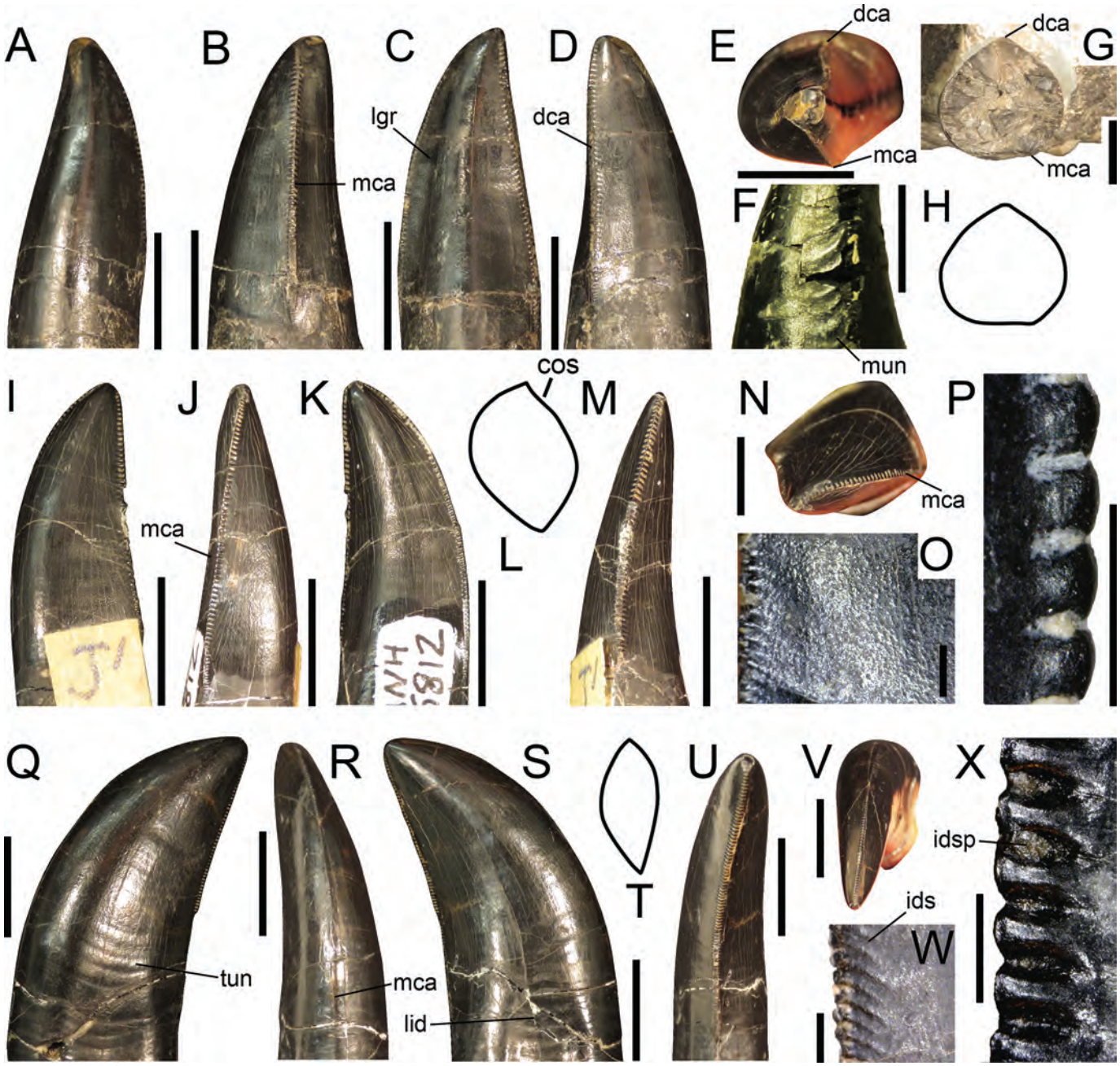

teeth have concave surfaces adjacent to the mesial and (or) distal carinae, conveying salinon- to J-shaped cross-sectional outlines to the crowns at the cervix (Fanti and Therrien 2007; Smith 2007; Hendrickx and Mateus 2014*a*; Hendrickx et al. 2020). However, the dentitions of *Majungasaurus* and most other abelisaurids clearly differ from those of *Sinraptor* and *Allosaurus* in the absence of twisted mesial carinae and labially deflected distal carinae in mesial and anterior lateral teeth. In addition, the distal denticles of abelisaurids such as *Kryptops*, *Majungasaurus*, and *Rugops* are apically hooked, and the tooth alveoli are typically subrectangular,

showing "en echelon dispositions" in the maxilla and dentary (Smith 2007; Hendrickx et al. 2020).

Characteristic dental features of *Sinraptor*

Enamel undulations, mesial carinae reaching the cervix, well-developed interdenticular sulci, and irregular enamel surface textures are relatively common dental features that are sometimes present in many distantly related theropod clades with ziphodont teeth (see Hendrickx et al. 2019). However, *Sinraptor dongi* exhibits two dental features whose distribution is relatively limited among non-maniraptoriform averostrans: (*i*) labial and lingual depressions at the bases of the crowns, resulting in figure-8-shaped cross-sectional outlines of the crowns at the cervix; and (*ii*) concave surfaces adjacent to the carinae on the labial and (or) lingual surfaces of lateral teeth. In non-maniraptoriform theropods, the presence of both labial and lingual depressions on some lateral crowns has been reported in the early ceratosaur *Berberosaurus* (Hendrickx et al. 2019) and in the tyrannosauroids *Alioramus* (Brusatte et al. 2012; Hendrickx et al. 2019), *Dilong* (Hendrickx et al. 2019), and *Proceratosaurus* (Rauhut et al. 2010). In allosauroids, these features have also been observed in the megaraptorans *Megaraptor* (Porfiri et al. 2014) and *Orkoraptor* (Novas et al. 2008) and in a few lateral teeth of *Allosaurus* (e.g., Natural History Museum of Utah, University of Utah, Salt Lake City, Utah (UMNH) VP 5841). Unlike in *Sinraptor dongi*, an figure-8-shaped cross section of the base of the crown is rare in *Allosaurus* because only a few maxillary and dentary crowns show a labial depression (C.Hendrickx, personal observation). Concave surfaces adjacent to the carinae can also be seen in the lateral dentition of several non-maniraptoriform theropods such as *Afrovenator*, *Dilophosaurus*, *Piatnitzkysaurus*, ceratosaurids, and most neovenatorids (Hendrickx et al. 2019). However, few theropods appear to have these concave surfaces adjacent to the distal carinae on both labial and lingual surfaces in multiple crowns, which is a feature that we have only observed in *Neovenator* (Dinosaur Isle, Isle of Wight Museum Services, Sandown, UK (MIWG) 6348).

Differentiating crowns along the jaw

Results of the discriminant analysis suggest that premaxillary, maxillary, and dentary teeth of *Sinraptor dongi* can be distinguished on the basis of quantitative data. However, this result should be considered with caution, given that only eight of the 29 maxillary teeth and seven of the 32 dentary teeth could be sampled. In addition, only the CBL and the CBW of four of the eight premaxillary teeth were measured. Maxillary and dentary teeth are difficult to differentiate in *Coelophysis* (Buckley and Currie 2014) and tyrannosaurids (Samman et al. 2005; Buckley et al. 2010). This would also be expected in *Sinraptor dongi* if teeth from both sides of the jaw and from a wider positional range were included in this study. However, there is little doubt that the premaxillary teeth of *Sinraptor dongi* can be distinguished from lateral maxillary and dentary teeth and possibly even from mesial dentary teeth. This hypothesis, however, needs to be tested with a broader sample of teeth.

Feeding ecology

If the dentition of *Sinraptor dongi* is obviously adapted for a carnivorous diet, several features suggest that its teeth were suited for a predatory lifestyle. Similar to those of abelisaurids and tyrannosaurids, the mesial teeth of *Sinraptor dongi* and *Allosaurus* are mesiodistally thick and were able to endure high mechanical stresses (Hendrickx et al. 2019). Robust mesial dentition appears to be adapted towards diets involving bone crunching and bone biting, with high degrees of torsion applied on mesial teeth (Reichel 2010, 2012). Such a mesial dentition was suited for gripping and pulling on prey in a bite-and-hold manner (Sampson and Witmer 2007; Reichel 2012). If mesial teeth with lingually deflected carinae and D- and U-shaped cross sections are perfectly suited for defleshing carcasses (Reichel 2012), the wide distances between mesial and distal carinae in mesial teeth, associated with spiralling mesial carinae and deflected distal carinae in anterior lateral teeth, would make wide cuts, keeping the wounds open and ultimately causing fatal injuries to the prey (Bakker 1998; Reichel 2012; Hendrickx et al. 2019). Additional evidence supports *Sinraptor dongi* as a predator. The large number of partially healed bite wounds seen on the cranial material of *Sinraptor dongi* (i.e., 28 tooth strike lesions distributed on the maxilla, jugal, dentary, prearticular, and possibly the surangular; Tanke and Currie 1998; Fig. 2B) was interpreted by Tanke and Currie (1998) to be indicative of aggressive inter- or intraspecific biting. Because *Sinraptor dongi* appears to be the only large-bodied theropod from the upper beds of the Shishugou Formation, intraspecific head- and face-biting behaviour most likely occurred in this taxon. If true, this supports the fact that the dentition of *Sinraptor dongi* was capable of enduring tooth-to-bone contact and was consequently well suited to a predatory lifestyle. Indeed, extensive spalled surfaces on the crown apices, which reflect flaking of enamel caused by the contact between the crown and food (Schubert and Ungar 2005), combined with fully worn apices in some mesial and lateral teeth, clearly indicate particularly high forces produced during contact with what was most likely the bones of prey items. *Sinraptor dongi*, together with *Allosaurus*, have been hypothesized to be "strike-and-tear/pull feeders", rapidly striking downwards at smaller prey using the mesial dentition (Snively and Russell 2007). Neck muscle morphologies in *Sinraptor dongi* and *Allosaurus* correlate with powerful ventroflexise kinematics, which would facilitate cutting flesh with the upper dentition (Snively and Russell 2007). *Allosaurus*, whose dentition is very similar to that of *Sinraptor dongi*, is widely regarded as a predator on the basis of the discovery of a *Stegosaurus* cervical plate with a bite pattern matching that of *Allosaurus*, and an *Allosaurus* caudal vertebra showing a partially healed wound likely caused by a *Stegosaurus* tail spike (Carpenter et al. 2005). Consequently, *Sinraptor dongi* is here interpreted as a predator, likely having preyed on medium-sized herbivorous dinosaurs such as the stegosaurid *Jiangjunosaurus junggarensis*, using its dentition to inflict fatal injuries in a manner similar to that of *Allosaurus*.

Conclusions

By describing in detail the dentition of *Sinraptor dongi*, this study reveals the presence of a suite of dental features restricted to this taxon. The mesial dentition of *Sinraptor* is made of labiolingually thick crowns in which the mesial carina twists mesiolingually to reach the cervix. The lingual surfaces of mesial teeth display one or more mesiodistally concave surfaces adjacent to the carinae for the entire CH. The lateral crowns typically show weakly to strongly labially deflected distal carinae, centrally positioned to slightly twisted mesial carinae reaching the cervix, and flat to mesiodistally concave surfaces centrally positioned on the bases of the crowns on both labial and lingual surfaces. The dentitions of *Allosaurus* and *Sinraptor* are particularly similar, differing only in the labiolingual compression of the lateral crowns and in the number of premaxillary teeth. Both allosauroid taxa have a dentition adapted for a predatory lifestyle, including robust premaxillary teeth with widely separated mesial and distal carinae and anterior lateral crowns with mesiolingually twisted mesial carinae and labially deflected distal carinae. The mesial dentition of non-carcharodontosaurian allosauroids was well suited for gripping and pulling on prey in a bite-and-hold manner, whereas both mesial and anterior lateral teeth were capable of inflicting wide cuts and open wounds, which led to profuse bleeding in the prey.

This comprehensive description of the dentition of *Sinraptor* supplements those for *Coelophysis* (Buckley and Currie 2014), *Majungasaurus* (Smith 2007), Abelisauridae (Hendrickx et al. 2020), Megalosauridae (Hendrickx et al. 2015*b*), *Tyrannosaurus* (Smith 2005), *Troodon* (Currie 1987; Currie et al. 1990), *Buitreraptor*

(Gianechini et al. 2011), and *Dromaeosaurus* (Currie et al. 1990). These descriptions account for fewer than 10% of non-avian theropods with well-preserved dental material. The dentitions of most theropods indeed suffer from poorly detailed descriptions, which is why identification of the shed teeth of theropods, abundantly represented at dinosaur fossil sites, can only be assigned to more inclusive clades. This work aims to encourage other authors to provide a comprehensive description of the dentition of theropods, with details on tooth cross sections, denticle morphologies, and crown ornamentations, among others.

Acknowledgements

We are particularly thankful to Li Feng (IVPP), Hui Ouyang (Chongqing Museum of Natural History, Chongqing, China (CV)), Tao Jiang (CV), Guang-Zhao Peng (Zigong Dinosaurian Museum, Zigong, Sichuan, China (ZDM)), Shan Jiang (ZDM), Dong Zhiming (Lufeng World Dinosaur Valley Park, Yunnan, China (ZLJ)), Tao Wang (ZLJ), Octávio Mateus (Museu da Lourinhã, Lourinhã, Portugal (ML)), Simão Mateus (ML), Hans-Jacob Siber (Sauriermuseum Aathal, Aathal, Switzerland), Ronan Allain (Muséum national d'Histoire naturelle, Paris, France), Sandra Chapman (Natural History Museum, London, UK (NHM)), Paul Barrett (NHM), Rodolfo Coria (Museo Municipal "Carmen Fuñes", Plaza Huincul, Argentina (MCF-PVPH)), Cecilia Succar (MCF-PVPH), Jorge Calvo (Centro Paleontológico Lago Barreales, Lago Barreales, Argentina), Juan D. Porfiri (Universidad Nacional del Comahue, Neuquén, Argentina), Juan Ignacio Canale (Museo de Ciencias Naturales de la Universidad Nacional de Comahue, Neuquén, Argentina), Fareed Krupp (Qatar Museums Authority, Doha, Qatar (QMA)), Khalid Hassan Al-Jaber (QMA), S.B Sanker (QMA), Paul Brinkman (North Carolina Museum of Natural Sciences, Raleigh, North Carolina (NCSM)), Lindsay Zanno (NCSM), Carrie Levitt-Bussian (Natural History Museum of Utah, University of Utah, Salt Lake City, Utah (UMNH)), Randall B. Irmis (UMNH), Matthew Carrano (Smithsonian National Museum of Natural History, Washington D.C. (NMNH)), Michael Brett-Surman (NMNH), Amanda Millhouse (NMNH), Daniel L. Brinkman (Yale Peabody Museum of Natural History, Yale University, New Haven, Connecticut), Paul Sereno (University of Chicago), Rodney Scheetz (Brigham Young University, Provo, Utah (BYU)), Brooks Britt (BYU), Matthew Lamanna (Carnegie Museum of Natural History, Pittsburgh, Pennsylvania (CMNH)), Amy Henrici (CMNH), Joe Sertich (Denver Museum of Nature & Science, Denver, Colorado (DMBH)), and Logan Ivy (DMNS) for access to specimens of *Sinraptor* and other allosauroid theropods and for their help provided during the visits to the collections. Special thanks go to Dong Zhiming and Tao Wang (ZLJ) for giving us access to an unpublished specimen and to Rafael Delcourt, Oliver Rauhut, Serjoscha Evers, Martín Ezcurra, Roger Benson, and Juan Canale for sharing photos of the dentition of allosauroids. We also thank Zichuan Qin for taking additional photos of the *Sinraptor* dentition at the IVPP, as well as reviewer Mike D'Emic and Associate Editor Craig Scott for their comments and suggestions, which significantly improved the quality of this work. We acknowledge the Willi Hennig Society and Øyvind Hammer for the use of TNT and Past3, respectively, as well as the paleoartists Scott Hartman, Gregory S. Paul, Cisiopurple, and T. Tischler for providing artwork and silhouettes of theropods on Phylopic or elsewhere. This research was supported by a Postdoctoral Fellowship from the University Research Committee of the University of the Witwatersrand to C.H. and National Science Foundation East Asia and Pacific Summer Institutes Office of International Science and Engineering 1311000 to J.S.

References

Bakker, R.T. 1998. Brontosaur killers: late Jurassic allosaurids as sabre-tooth cat analogues. Gaia, **15**: 145–158.

Brusatte, S.L., and Carr, T.D. 2016. The phylogeny and evolutionary history of tyrannosauroid dinosaurs. Scientific Reports, **6**: 20252. doi:10.1038/srep20252. PMID:26830019.

Brusatte, S.L., Benson, R.B.J., and Hutt, S. 2008. The osteology of *Neovenator salerii* (Dinosauria: Theropoda) from the Wealden Group (Barremian) of the Isle of Wight. Palaeontographical Society, **162**: 1–75.

Brusatte, S.L., Carr, T.D., and Norell, M.A. 2012. The osteology of *Alioramus*, a gracile and long-snouted tyrannosaurid (Dinosauria: Theropoda) from the Late Cretaceous of Mongolia. Bulletin of the American Museum of Natural History, **366**: 1–197. doi:10.1206/770.1.

Brusatte, S.L., Lloyd, G.T., Wang, S.C., and Norell, M.A. 2014. Gradual assembly of avian body plan culminated in rapid rates of evolution across the dinosaur-bird transition. Current Biology, **24**: 2386–2392. doi:10.1016/j.cub.2014.08.034. PMID:25264248.

Buckley, L.G., and Currie, P.J. 2014. Analysis of intraspecific and ontogenetic variation in the dentition of *Coelophysis bauri* (Late Triassic), and implications for the systematics of isolated theropod teeth. New Mexico Museum of Natural History and Science, **63**: 1–73.

Buckley, L.G., Larson, D.W., Reichel, M., and Samman, T. 2010. Quantifying tooth variation within a single population of *Albertosaurus sarcophagus* (Theropoda: Tyrannosauridae) and implications for identifying isolated teeth of tyrannosaurids. Canadian Journal of Earth Sciences, **47**(9): 1227–1251. doi:10.1139/E10-029.

Carpenter, K., Sanders, F., McWhinney, L.A., and Wood, L. 2005. Evidence for predator-prey relationships. *In* The carnivorous dinosaurs. *Edited by* K. Carpenter. Indiana University Press, Bloomington, Ind. pp. 325–350.

Carrano, M.T., Benson, R.B.J., and Sampson, S.D. 2012. The phylogeny of Tetanurae (Dinosauria: Theropoda). Journal of Systematic Palaeontology, **10**: 211–300. doi:10.1080/14772019.2011.630927.

Cau, A., Beyrand, V., Voeten, D.F.A.E., Fernandez, V., Tafforeau, P., Stein, K., et al. 2017. Synchrotron scanning reveals amphibious ecomorphology in a new clade of bird-like dinosaurs. Nature, **552**: 395–399. doi:10.1038/nature24679. PMID:29211712.

Choiniere, J.N., Clark, J.M., Forster, C.A., and Xu, X. 2010*a*. A basal coelurosaur (Dinosauria: Theropoda) from the Late Jurassic (Oxfordian) of the Shishugou Formation in Wucaiwan, People's Republic of China. Journal of Vertebrate Paleontology, **30**: 1773–1796. doi:10.1080/02724634.2010.520779.

Choiniere, J.N., Xu, X., Clark, J.M., Forster, C.A., Guo, Y., and Han, F. 2010*b*. A basal alvarezsauroid theropod from the Early Late Jurassic of Xinjiang, China. Science, **327**: 571–574. doi:10.1126/science.1182143. PMID:20110503.

Choiniere, J.N., Clark, J.M., Forster, C.A., Norell, M.A., Eberth, D.A., Erickson, G.M., et al. 2014*a*. A juvenile specimen of a new coelurosaur (Dinosauria: Theropoda) from the Middle–Late Jurassic Shishugou Formation of Xinjiang, People's Republic of China. Journal of Systematic Palaeontology, **12**: 177–215. doi:10.1080/14772019.2013.781067.

Choiniere, J.N., Clark, J.M., Norell, M., and Xu, X. 2014*b*. Cranial osteology of *Haplocheirus sollers* Choiniere et al., 2010 (Theropoda, Alvarezsauroidea). American Museum Novitates, **3816**: 1–44. doi:10.1206/3816.1.

Currie, P.J. 1987. Bird-like characteristics of the jaws and teeth of troodontid theropods (Dinosauria, Saurischia). Journal of Vertebrate Paleontology, **7**: 72–81. doi:10.1080/02724634.1987.10011638.

Currie, P.J. 1991. The Sino/Canadian Dinosaur Expeditions, 1986-1990. Geotimes, **36**: 18–21.

Currie, P.J., and Zhao, X.-J. 1993. A new carnosaur (Dinosauria, Theropoda) from the Jurassic of Xinjiang, People's Republic of China. Canadian Journal of Earth Sciences, **30**(10): 2037–2081. doi:10.1139/e93-179.

Currie, P.J., Rigby, J.K., Jr., and Sloan, R.E. 1990. Theropod teeth from the Judith River formation of southern Alberta, Canada. *In* Dinosaur systematics: approaches and perspectives. *Edited by* K. Carpenter and P.J. Currie. Cambridge University Press, New York, pp. 107–125.

Dong, Z. 1989. On a small ornithopod (*Gongbusaurus wucaiwanensis*) from Kelamaili, Jungar Basin, Xinjiang, China. Vertebrata PalAsiatica, **27**: 140–146.

Dong, Z. 1990. Sauropoda from the Kelameili Region of the Junggar Basin, Xinjiang Autonomous Region. Vertebrata PalAsiatica, **28**: 43–58.

Dong, Z. 1992. Sauropoda from the Kelameili Region of the Junggar Basin, Xinjiang Autonomous Region. Vertebrata PalAsiatica, **28**: 43–58.

Dong, Z. 1993. The field activities of the Sino-Canadian Dinosaur Project in China, 1987–1990. Canadian Journal of Earth Sciences, **30**(10): 1997–2001. doi:10.1139/e93-175.

Dong, Z., Russell, D.A., and Currie, P.J. 1988. The dinosaur project an international cooperative program on dinosaurs. Vertebrata PalAsiatica, **26**: 235–240.

Eberth, D.A., Xing, X., and Clark, J.M. 2010. Dinosaur death pits from the Jurassic of China. Palaios, **25**: 112–125. doi:10.2110/palo.2009.p09-028r.

Ezcurra, M. 2017. A new early coelophysoid neotheropod from the Late Triassic of Northwestern Argentina. Ameghiniana, **54**: 506–538. doi:10.5710/AMGH.04.08.2017.3100.

Fanti, F., and Therrien, F. 2007. Theropod tooth assemblages from the Late Cretaceous Maevarano Formation and the possible presence of dromaeosaurids in Madagascar. Acta Palaeontologica Polonica, **52**: 155–166.

Gauthier, J. 1986. Saurischian monophyly and the origin of birds. *In* The origin of birds and the evolution of flight. *Edited by* K. Padian. Memoirs of the California Academy of Sciences Number 8, San Francisco, California, pp. 1–55.

Gerke, O., and Wings, O. 2016. Multivariate and cladistic analyses of isolated

teeth reveal sympatry of theropod dinosaurs in the Late Jurassic of Northern Germany. PLoS ONE, **11**: e0158334. doi:10.1371/journal.pone.0158334. PMID: 27383054.

Gianechini, F.A., Makovicky, P.J., and Apesteguía, S. 2011. The teeth of the unenlagiine theropod *Buitreraptor* from the Cretaceous of Patagonia, Argentina, and the unusual dentition of the Gondwanan dromaeosaurids. Acta Palaeontologica Polonica, **56**: 279–290. doi:10.4202/app.2009.0127.

Goloboff, P.A., Farris, J.S., Källersjö, M., Oxelman, B., Ramírez, M.J., and Szumik, C.A. 2003. Improvements to resampling measures of group support. Cladistics, **19**: 324–332. doi:10.1016/S0748-3007(03)00060-4.

Goloboff, P.A., Farris, J.S., and Nixon, K.C. 2008. TNT, a free program for phylogenetic analysis. Cladistics, **24**: 774–786. doi:10.1111/j.1096-0031.2008.00217.x.

Hammer, Ø., Harper, D.A.T., and Ryan, P.D. 2001. Past: paleontological Statistics Software Package for education and data analysis. Palaeontologia Electronica, **4**: 1–9.

Han, F., Clark, J.M., Xu, X., Sullivan, C., Choiniere, J., and Hone, D.W.E. 2011. Theropod teeth from the Middle-Upper Jurassic Shishugou Formation of northwest Xinjiang, China. Journal of Vertebrate Paleontology, **31**: 111–126. doi:10.1080/02724634.2011.546291.

Han, F., Forster, C.A., Clark, J.M., and Xu, X. 2015. A new taxon of basal ceratopsian from China and the early evolution of Ceratopsia. PLoS ONE, **10**: e0143369. doi:10.1371/journal.pone.0143369. PMID:26649770.

Han, F., Forster, C.A., Clark, J.M., and Xu, X. 2016. Cranial anatomy of *Yinlong downsi* (Ornithischia: Ceratopsia) from the Upper Jurassic Shishugou Formation of Xinjiang, China. Journal of Vertebrate Paleontology, **36**: e1029579. doi:10.1080/02724634.2015.1029579.

Han, F., Forster, C.A., Xu, X., and Clark, J.M. 2018. Postcranial anatomy of *Yinlong downsi* (Dinosauria: Ceratopsia) from the Upper Jurassic Shishugou Formation of China and the phylogeny of basal ornithischians. Journal of Systematic Palaeontology, **16**: 1159–1187. doi:10.1080/14772019.2017.1369185.

Hendrickx, C., and Mateus, O. 2014*a*. Abelisauridae (Dinosauria: Theropoda) from the Late Jurassic of Portugal and dentition-based phylogeny as a contribution for the identification of isolated theropod teeth. Zootaxa, **3759**: 1–74. doi:10.11646/zootaxa.3759.1.1. PMID:24869965.

Hendrickx, C., and Mateus, O. 2014*b*. *Torvosaurus gurneyi* n. sp., the largest terrestrial predator from Europe, and a proposed terminology of the maxilla anatomy in nonavian theropods. PLoS ONE, **9**: e88905. doi:10.1371/journal.pone.0088905. PMID:24598585.

Hendrickx, C., Hartman, S.A., and Mateus, O. 2015*a*. An overview of non-avian theropod discoveries and classification. PalArch's Journal of Vertebrate Palaeontology, **12**: 1–73.

Hendrickx, C., Mateus, O., and Araújo, R. 2015*b*. The dentition of Megalosauridae (Theropoda: Dinosauria). Acta Palaeontologica Polonica, **60**: 627–642. doi:10.4202/app.00056.2013.

Hendrickx, C., Mateus, O., and Araújo, R. 2015*c*. A proposed terminology of theropod teeth (Dinosauria, Saurischia). Journal of Vertebrate Paleontology, **35**: e982797. doi:10.1080/02724634.2015.982797.

Hendrickx, C., Mateus, O., Araújo, R., and Choiniere, J. 2019. The distribution of dental features in non-avian theropod dinosaurs: Taxonomic potential, degree of homoplasy, and major evolutionary trends. Palaeontologia Electronica, **22**: 1–110. doi:10.26879/820.

Hendrickx, C., Tschopp, E., and Ezcurra, M.D. 2020. Taxonomic identification of isolated theropod teeth: the case of the shed tooth crown associated with *Aerosteon* (Theropoda: Megaraptora) and the dentition of Abelisauridae. Cretaceous Research, **108**: 104312. doi:10.1016/j.cretres.2019.104312.

Howgate, M.E. 1984. The teeth of *Archaeopteryx* and a reinterpretation of the Eichstätt specimen. Zoological Journal of the Linnean Society, **82**: 159–175. doi:10.1111/j.1096-3642.1984.tb00540.x.

Jia, C., Foster, C.A., Xing, X.U., and Clark, J.M. 2007. The first stegosaur (Dinosauria, Ornithischia) from the Upper Jurassic Shishugou Formation of Xinjiang, China. Acta Geologica Sinica (English Edition), **81**: 351–356. doi:10.1111/j.1755-6724.2007.tb00959.x.

Langer, M.C., Ezcurra, M.D., Rauhut, O.W.M., Benton, M.J., Knoll, F., McPhee, B.W., et al. 2017. Untangling the dinosaur family tree. Nature, **551**: E1–E3. doi:10.1038/nature24011.

Lloyd, G.T. 2016. Estimating morphological diversity and tempo with discrete character-taxon matrices: implementation, challenges, progress, and future directions. Biological Journal of the Linnean Society, **118**: 131–151. doi:10.1111/bij.12746.

Loewen, M.A. 2010. Variation in the Late Jurassic theropod dinosaur *Allosaurus*: ontogenetic, functional, and taxonomic implications. Ph.D. dissertation, The University of Utah, Utah.

Maddison, W.P., and Maddison, D.R. 2017. Mesquite: a modular system for evolutionary analysis. Version 3.2. Available from http://mesquiteproject.org [accessed 16 June 2017].

Madsen, J.H. 1976. *Allosaurus fragilis*: a revised osteology. Utah Geological Survey Bulletin, **109**: 1–177.

Marsh, O.C. 1878. Principal characters of American Jurassic dinosaurs, Part I. American Journal of Science Series 3, **16**: 411–416. doi:10.2475/ajs.s3-16.95.411.

Marsh, O.C. 1881. Principal characters of American Jurassic dinosaurs, Part V. American Journal of Science Series 3, **21**: 417–423. doi:10.2475/ajs.s3-21.125.417.

Meyer, H.V. 1861. *Archaeopteryx lithographica* (Vogel-Feder) und *Pterodactylus* von Solnhofen. Neues Jahrbuch für Mineralogie, Geognosie, Geologie und Petrefakten-Kunde, **1861**: 678–679.

Moore, A.J., Mo, J., Clark, J.M., and Xu, X. 2018. Cranial anatomy of *Bellusaurus sui* (Dinosauria: Eusauropoda) from the Middle-Late Jurassic Shishugou Formation of northwest China and a review of sauropod cranial ontogeny. PeerJ, **6**: e4881. doi:10.7717/peerj.4881. PMID:29868283.

Moore, M.K. 2013. Chapter 4 - Sex estimation and assessment. *In* Research methods in human skeletal biology. *Edited by* E.A. DiGangi and M.K. Moore. Academic Press, pp. 91–116. doi:10.1016/B978-0-12-385189-5.00004-2.

Müller, R.T., Langer, M.C., Bronzati, M., Pacheco, C.P., Cabreira, S.F., and Dias-Da-Silva, S. 2018. Early evolution of sauropodomorphs: anatomy and phylogenetic relationships of a remarkably well-preserved dinosaur from the Upper Triassic of southern Brazil. Zoological Journal of the Linnean Society, **184**: 1187–1248. doi:10.1093/zoolinnean/zly009.

Nixon, K.C. 2002. WinClada, version 1.00.08. Ithaca, New York. [Published by the author.]

Novas, F.E., Ezcurra, M.D., and Lecuona, A. 2008. *Orkoraptor burkei* nov. gen. et sp., a large theropod from the Maastrichtian Pari Aike Formation, Southern Patagonia, Argentina. Cretaceous Research, **29**: 468–480. doi:10.1016/j.cretres.2008.01.001.

Owen, R. 1842. Report on British fossil reptiles. Report of the British Association for the Advancement of Science, **11**(1841): 60–294.

Paul, G.S. 1988. Predatory dinosaurs of the world: a complete illustrated guide. Simon & Schuster.

Paul, G.S. (*Editor*). 2010. Dinosaurs: a field guide. A&C Black.

Porfiri, J.D., Novas, F.E., Calvo, J.O., Agnolín, F.L., Ezcurra, M.D., and Cerda, I.A. 2014. Juvenile specimen of *Megaraptor* (Dinosauria, Theropoda) sheds light about tyrannosauroid radiation. Cretaceous Research, **51**: 35–55. doi:10.1016/j.cretres.2014.04.007.

Qin, Z., Clark, J., Choiniere, J., and Xu, X. 2019. A new alvarezsaurian theropod from the Upper Jurassic Shishugou Formation of western China. Scientific Reports, **9**: 1–14. doi:10.1038/s41598-019-48148-7. PMID:31409823.

Rauhut, O.W.M. 2004. Provenance and anatomy of *Genyodectes serus*, a large-toothed ceratosaur (Dinosauria: Theropoda) from Patagonia. Journal of Vertebrate Paleontology, **24**: 894–902. doi:10.1671/0272-4634(2004)024[0894:PAAOGS]2.0.CO;2.

Rauhut, O.W.M. 2014. New observations on the skull of *Archaeopteryx*. Paläontologische Zeitschrift, **88**: 211–221. doi:10.1007/s12542-013-0186-0.

Rauhut, O.W.M., and Carrano, M.T. 2016. The theropod dinosaur *Elaphrosaurus bambergi* Janensch, 1920, from the Late Jurassic of Tendaguru, Tanzania. Zoological Journal of the Linnean Society, **178**: 546–610. doi:10.1111/zoj.12425.

Rauhut, O.W.M., Milner, A.C., and Moore-Fay, S. 2010. Cranial osteology and phylogenetic position of the theropod dinosaur *Proceratosaurus bradleyi* (Woodward, 1910) from the Middle Jurassic of England. Zoological Journal of the Linnean Society, **158**: 155–195. doi:10.1111/j.1096-3642.2009.00591.x.

Rauhut, O.W.M., Foth, C., Tischlinger, H., and Norell, M.A. 2012. Exceptionally preserved juvenile megalosauroid theropod dinosaur with filamentous integument from the Late Jurassic of Germany. Proceedings of the National Academy of Sciences, **109**: 11746–11751. doi:10.1073/pnas.1203238109.

Rauhut, O.W., Hübner, T., and Lanser, K.-P. 2016. A new megalosaurid theropod dinosaur from the late Middle Jurassic (Callovian) of north-western Germany: implications for theropod evolution and faunal turnover in the Jurassic. Palaeontologia Electronica, **19**: 1–65. doi:10.26879/654.

Rauhut, O.W.M., Foth, C., and Tischlinger, H. 2018. The oldest *Archaeopteryx* (Theropoda: Avialiae): a new specimen from the Kimmeridgian/Tithonian boundary of Schamhaupten, Bavaria. PeerJ, **6**: e4191. doi:10.7717/peerj.4191. PMID:29383285.

Reichel, M. 2010. The heterodonty of *Albertosaurus sarcophagus* and *Tyrannosaurus rex*: biomechanical implications inferred through 3-D models. Canadian Journal of Earth Sciences, **47**(9): 1253–1261. doi:10.1139/E10-063.

Reichel, M. 2012. The variation of angles between anterior and posterior carinae of tyrannosaurid teeth. Canadian Journal of Earth Sciences, **49**(3): 477–491. doi:10.1139/e11-068.

Richter, U., Mudroch, A., and Buckley, L.G. 2013. Isolated theropod teeth from the Kem Kem Beds (Early Cenomanian) near Taouz, Morocco. Paläontologische Zeitschrift, **87**: 291–309. doi:10.1007/s12542-012-0153-1.

Russell, D.A., and Zheng, Z. 1993. A large mamenchisaurid from the Junggar Basin, Xinjiang, People's Republic of China. Canadian Journal of Earth Sciences, **30**(10): 2082–2095. doi:10.1139/e93-180.

Samman, T., Powell, G.L., Currie, P.J., and Hills, L.V. 2005. Morphometry of the teeth of western North American tyrannosaurids and its applicability to quantitative classification. Acta Palaeontologica Polonica, **50**: 757–776.

Sampson, S.D., and Witmer, L.M. 2007. Craniofacial anatomy of *Majungasaurus crenatissimus* (Theropoda: Abelisauridae) from the Late Cretaceous of Madagascar. Journal of Vertebrate Paleontology, **27**: 32–104. doi:10.1671/0272-4634(2007)27[32:CAOMCT]2.0.CO;2.

Schubert, B.W., and Ungar, P.S. 2005. Wear facets and enamel spalling in tyrannosaurid dinosaurs. Acta Palaeontologica Polonica, **50**: 93–99.

Seeley, H.G. 1887. I. On the classification of the fossil animals commonly named Dinosauria. Proceedings of the Royal Society of London, **43**: 165–171. doi:10.1098/rspl.1887.0117.

Sereno, P.C., and Novas, F.E. 1992. The complete skull and skeleton of an early

dinosaur. Science, **258**: 1137–1140. doi:10.1126/science.258.5085.1137. PMID: 17789086.

Sereno, P.C., and Novas, F.E. 1994. The skull and neck of the basal theropod *Herrerasaurus ischigualastensis*. Journal of Vertebrate Paleontology, **13**: 451–476. doi:10.1080/02724634.1994.10011525.

Smith, J.B. 2005. Heterodonty in *Tyrannosaurus rex*: implications for the taxonomic and systematic utility of theropod dentitions. Journal of Vertebrate Paleontology, **25**: 865–887. doi:10.1671/0272-4634(2005)025[0865:HITRIF]2.0.CO;2.

Smith, J.B. 2007. Dental morphology and variation in *Majungasaurus crenatissimus* (Theropoda: Abelisauridae) from the Late Cretaceous of Madagascar. Journal of Vertebrate Paleontology, **27**: 103–126. doi:10.1671/0272-4634(2007)27[103:DMAVIM]2.0.CO;2.

Smith, J.B., and Dodson, P. 2003. A proposal for a standard terminology of anatomical notation and orientation in fossil vertebrate dentitions. Journal of Vertebrate Paleontology, **23**: 1–12. doi:10.1671/0272-4634(2003)23[1:APFAST]2.0.CO;2.

Smith, J.B., Vann, D.R., and Dodson, P. 2005. Dental morphology and variation in theropod dinosaurs: implications for the taxonomic identification of isolated teeth. The Anatomical Record Part A: Discoveries in Molecular, Cellular, and Evolutionary Biology, **285**: 699–736. doi:10.1002/ar.a.20206. PMID:15986487.

Snively, E., and Russell, A.P. 2007. Functional variation of neck muscles and their relation to feeding style in Tyrannosauridae and other large theropod dinosaurs. The Anatomical Record: Advances in Integrative Anatomy and Evolutionary Biology, **290**: 934–957. doi:10.1002/ar.20563.

Tanke, D.H., and Currie, P.J. 1998. Head-biting behavior in theropod dinosaurs: Paleopathological evidence. Gaia, **15**: 167–184. doi:10.7939/R34T6FJ1P.

Wang, S., Stiegler, J., Amiot, R., Clark, J.M., Balanoff, A.M., and Xu, X. 2016. Cranial ontogenetic variation in the Late Jurassic Chinese ceratosaur *Limusaurus inextricabilis*. *In* 76th Annual Meeting Society of Vertebrate Paleontology, Salt Lake City, Utah, USA. (October 26–29, 2016), Program and Abstracts. *Edited by* A.A. Farke, A. MacKenzie, and J. Miller-Camp. 246 pp.

Wang, S., Stiegler, J., Amiot, R., Wang, X., Du, G., Clark, J.M., and Xu, X. 2017. Extreme ontogenetic changes in a ceratosaurian theropod. Current Biology, **27**: 144–148. doi:10.1016/j.cub.2016.10.043. PMID:28017609.

Williamson, T.E., and Brusatte, S.L. 2014. Small theropod teeth from the Late Cretaceous of the San Juan Basin, Northwestern New Mexico and their implications for understanding Latest Cretaceous dinosaur evolution. PLoS ONE, **9**: e93190. doi:10.1371/journal.pone.0093190. PMID:24709990.

Xu, X., and Clark, J.M. 2008. The presence of a gigantic theropod in the Jurassic Shishugou Formation, Junggar Basin, western China. Vertebrata PalAsiatica, **46**: 57–160.

Xu, X., Clark, J.M., Forster, C.A., Norell, M.A., Erickson, G.M., Eberth, D.A., et al. 2006*a*. A basal tyrannosauroid dinosaur from the Late Jurassic of China. Nature, **439**: 715–718. doi:10.1038/nature04511. PMID:16467836.

Xu, X., Forster, C.A., Clark, J.M., and Mo, J. 2006*b*. A basal ceratopsian with transitional features from the Late Jurassic of northwestern China. Proceedings of the Royal Society B: Biological Sciences, **273**: 2135–2140. doi:10.1098/rspb.2006.3566. PMID:16901832.

Xu, X., Clark, J.M., Mo, J., Choiniere, J., Forster, C.A., Erickson, G.M., et al. 2009. A Jurassic ceratosaur from China helps clarify avian digital homologies. Nature, **459**: 940–944. doi:10.1038/nature08124. PMID:19536256.

Xu, X., Choiniere, J., Tan, Q., Benson, R.B.J., Clark, J., Sullivan, C., et al. 2018. Two Early Cretaceous fossils document transitional stages in alvarezsaurian dinosaur evolution. Current Biology, **28**: 1–8. doi:10.1016/j.cub.2018.07.057. PMID: 30146153.

Young, C.C. 1937. A new dinosaurian from Sinkiang. Palaeontologia Sinica, Series C, **2**: 1–29.

Young, C.M.E., Hendrickx, C., Challands, T.J., Foffa, D., Ross, D.A., Butler, I.B., and Brusatte, S.L. 2019. New theropod dinosaur teeth from the Middle Jurassic of the Isle of Skye, Scotland. Scottish Journal of Geology, **55**: 7–19. doi:10.1144/sjg2018-020.